Inference of Locally Varying Anisotropy Fields

by

Maksuda Lillah

A thesis submitted in partial fulfillment of the requirements for the degree of

Master of Science
in
Mining Engineering

Department of Civil and Environmental Engineering
University of Alberta

Abstract

Considering nonstationary features in geostatistical modeling is important. Recent developments in nonlinear estimation provide a practical way to infuse geological realism into numerical modeling by incorporating complex spatial features. Second order nonstationarity when present must be considered for more accurate geo-models. A critical step when considering second order nonstationarity is a parametric representation of the underlying anisotropy field quantifying the orientation and magnitude of anisotropy exhaustively. The inference of a locally varying anisotropy (LVA) field is deposit and data specific and this work presents a suit of methodologies for field generation in both 2D and 3D cases. Three different data types are explored: (1) 3D point data from direct angle measures from down bore hole formation etc, (2) exhaustive data from outcrop images, (3) compact geologic bodies typically inferred by geologists. Proposed methodologies for the generation of LVA field include reorienting point data by angle variance criteria and estimation by kriging, interpolating orientation in 3D by quaternion averaging, identifying local structures from exhaustive data by moving window technique and centerline extraction of geo bodies by thinning. Features of interest can occur at a coarser or finer scale than the grid size of the final model. Local structures of LVA can be better captured by allowing search areas to adjust to the range of the relevant features. In deposits characterized by varying scales of anisotropy, adaptive moving windows are used to assess the local orientation. Usually several different data types may need to be consolidated for the generation of a single LVA field and a tensor based combination scheme is discussed whereby multiple LVA fields can be merged. In the last section, data from a copper porphyry deposit is considered for LVA generation and results show higher correlation and lower mean squared error in cross validation analysis when kriging with LVA compared to traditional kriging.

Acknowledgements

This dissertation would not be possible without the guidance and support of my supervisor Dr. Jeff Boisvert. Dr. Clayton Deutsch had many inputs throughout the process and for that I am grateful. I would also like to thank the member companies at CCG for providing the financial support needed to complete this work.

My family deserves a special mention. They all mean the world to me and I would not be here without their constant love and encouragement. Lastly I dedicate this thesis to the loving memories of my grandfather.

Contents

List of Tables

List of Figures

List of Symbols

α	strike angle
β	dip angle
ϕ	plunge angle
$\gamma(\mathbf{h})$	variogram function
σ^2	variance
σ^2_{sp}	spherical angle variance
λ	eigenvalue
A	local neighbourhood
$a(\mu_0)$	unit vector
a_x	range of anisotropy in X direction
a_y	range of anisotropy in Y direction
a_z	range of anisotropy in Z direction
$C(\mathbf{h})$	covariance between points seperated by textbfh
D_k	discrete differenciating operator
d	dimensionless distance
d	distance matrix
d_x	seperation distance in X direction
d_y	seperation distance in Y direction
d_z	seperation distance in Z direction
E	expected value
$F()$	gaussian filter
$g(\mathbf{u})$	gradient field
M	a 4×4 matrix containing average attitude
m	mean
q_i	unit quaternion
R	reliability
R_α	rotation matrix
$R_(q, \theta)$	Euler rotation angle
r_1	ratio of minor to major directions of anisotropy
r_2	ratio of vertical to major directions of anisotropy
S	angle stability
T	structure tensor
U_N	normalized averaged tensor
X	axis of orientation
$\bar{x}$	mean orientation
x^o	spherical angle
$Z(\mathbf{u})$	regionalized random variable

Chapter 1

Introduction

Curvilinear geology such as fluvial channel belts, braided river systems, veins, folded outcrops etc are difficult to model with standard geostatistical techniques. Traditional kriging can only consider a single direction of anisotropy but this assumption is inappropriate for reproducing many non-linear structures. One methodology is to incorporate a locally varying anisotropy (LVA) field into estimation. LVA fields parameterize the orientation and magnitude of anisotropy at all locations in a modeling domain. There has been interest to incorporate these exhaustive vector maps into geostatistical techniques so complex geological formations are reproduced with accuracy: Deutsch and Lewis (1992), Xu (1996) implemented kriging with local search; Stroet and Snepvangers (2005) directly calculates local orientation from data; and recently Boisvert and Deutsch (2011) use non-linear distance paths to tie LVA into kriging.

Spatial interactions between locations in the presence of anisotropy show maximum connectedness along a path defined by anisotropy orientation which may arise due to natural processes during formation. This information, when available, must be taken into account as feature architectures, petro physical property behaviour and boundary modeling across surfaces can be better reproduced to closely match the actual geology. Accurate modeling can have far reaching effects for resource volumes prediction, reservoir heterogeneities characterization, mine planning and design etc. Several reasonable techniques have been developed that relax second order stationary assumptions but requires a well defined anisotropy field. LVA fields can be utilized in tandem with estimation such as kriging, or in a simulation framework.

Anisotropy refers to properties in geological formations that show preferential directions of continuity, i.e. properties are more continuous in one direction than in another. Often the spatial continuity of properties are complex, non - linear structures e.g. porosity and permeability in clastic rocks and fluvial reservoirs, overturned folding, non - linear fault lines etc. These struc-

tures are marked with varied continuities in many directions and their modeling is difficult with traditional methods since typical geostatistical tools do not account for locally varying directions of anisotropy.

Increasingly, geostatistics is becoming more concerned with the assumption of second order stationarity - the assumption that covariance function between a set of fixed locations is translation invariant. First order non-stationarity implies the mean of a regionalized random variable ($Z(\mathbf{u})$) is not constant and the condition can be accounted for by introducing a locally varying mean into modeling. On the other hand moving away from second order stationarity is non-trivial. A solution is to parameterize LVA directions of continuity at all locations within the domain. This LVA field describes the magnitude and direction of anisotropy of the property of interest. Information from the LVA field can be used to give increased accuracy and realism in modeling complex geometries. Consider the outcrop image (Figure 1.1) with the LVA orientations following the contours along the folded seams. This example shows the need to consider non-stationarity as the local covariance is clearly not constant.

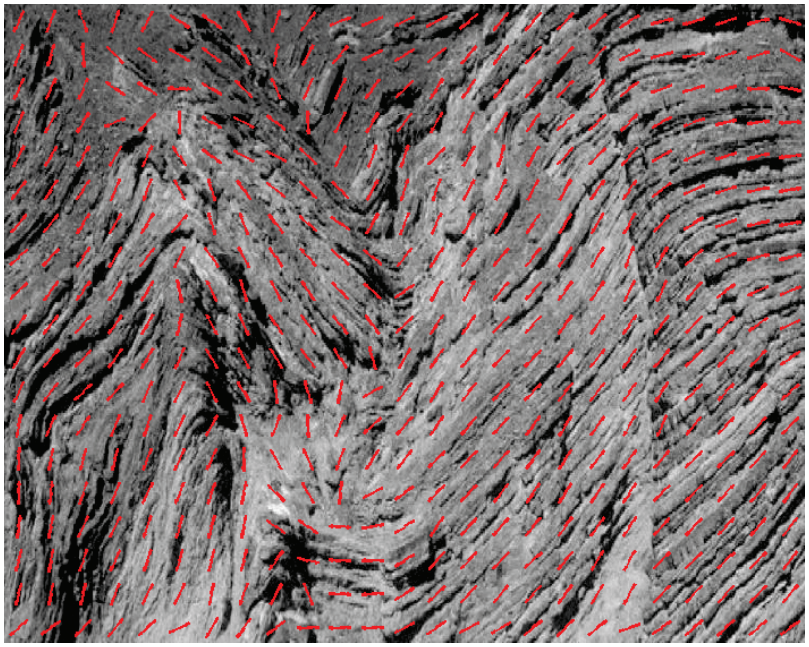

Figure 1.1: Folded outcrop of dimension 594×780 units showing anisotropy. LVA orientations are overlain and follow the geologic continuity of the deposit. Greyscale image source: http://gsfc.nasa.gov/Sect2/Sect2_1a.html

1.1 Background

The LVA field completely describes the direction of continuity and magnitude of anisotropy in the modeling domain. An exhaustive LVA field is parameterized by three angles which together describe the major direction of continuity and two ratios r_1, r_2. The magnitude of anisotropy is the ratio of the major and minor ranges. In 3D the anisotropy orientation is completely given by strike, dip and plunge angles and two ratios taken with respect to the range in the major direction: r_1 = minor/major, r_2 = vert/major (Boisvert, 2010). For 2D only the strike angle and r_1 are needed (Figure 1.2).

Geometric anisotropy can be illustrated by first considering an isotropic case represented by a sphere and the transformations (rotation and axis scaling) that are needed to define an ellipsoid (Deutsch and Journel, 1998). In 2D the spatial anisotropy is described by an ellipse where the major axis describes the principal direction of continuity and the minor axis corresponds to the minimum direction of continuity. The elliptical contour of anisotropy visually illustrates the locus of points that are equidistant from a central node in considering a covariance function, often termed the anisotropic distance. So, mathematically the directional ranges represented as the semi -major and semi -minor axes of the ellipse and can be calculated for any orientation. Once the major direction of anisotropy is determined the original (spatial) coordinate system is rotated to align with actual geologic continuity. The new coordinate system $X'Y'$ (Figure 1.2) is scaled to account for the magnitude of anisotropy and the procedure allows to calculate a dimensionless anisotropic distance between any two locations (Equation 1.1).

Consider two points in space separated by distance d, then this Cartesian distance in the original coordinate system must be scaled to account for anisotropy. The ranges of anisotropy are given by a_x, a_y, a_z and ($dx\ dy\ dz$) are the separation distances in the original coordinate system (Leuangthong et al, 2008). The actual anisotropic distance vector (d) along the path related by anisotropy is calculated as:

$$d = \sqrt{(\frac{dx}{a_x})^2 + (\frac{dy}{a_y})^2 + (\frac{dz}{a_z})^2} \tag{1.1}$$

The direction of maximum continuity is specified by the rotated vector $\mathbf{d_R}$ so it aligns with the given structural continuity to give the scalar distance d, which is used to calculate the covariance often from a variogram model of the deposit. The reason for considering the scalar d is that physical process such as weathering, sedimentation, erosion etc lead to preferential degrees of continuity in depositions and points that lie along the direction of anisotropy have stronger correlation in the

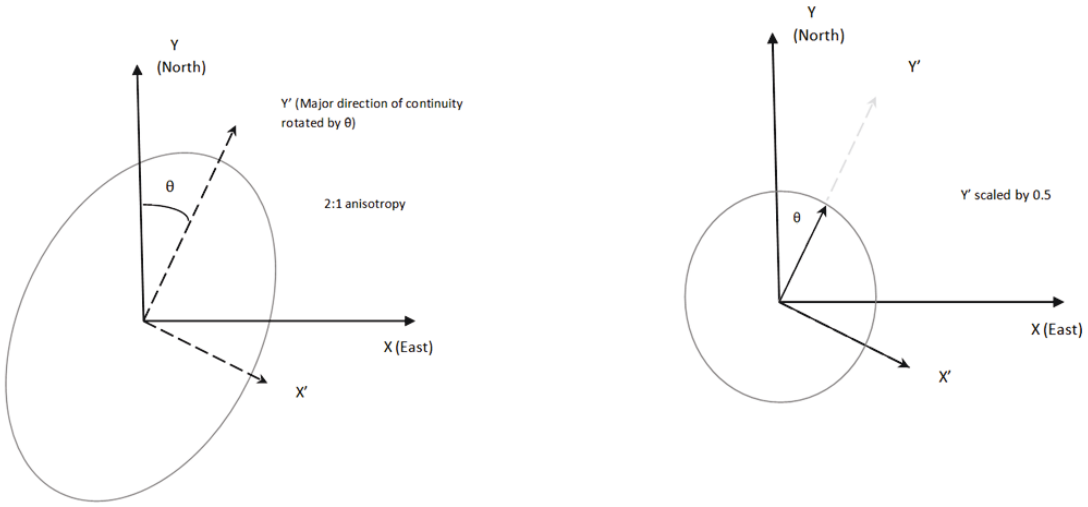

Figure 1.2: Representation of the parameters needed to define anisotropy in 2D. Strike is always taken clockwise from the positive North axis. The original coordinate system (left) is scaled to get an isotropic coordinate system (right), represented by an ellipse and circle respectively.

specified direction than in any other (Boisvert, 2010). When estimating at an unknown location using traditional methods such as kriging, points along the direction of anisotropy are given higher weights since they are 'closer' in terms of the anisotropic distance.

1.1.1 Parameterization of LVA field

The LVA field describes the orientation and magnitude in the domain. In 2D the angle from the azimuth and the ratio of minor and major directions are needed to define anisotropy. As seen in the previous sections, information from LVA orientations are coded to anisotropic distances before estimation is considered. For two points separated by distance vector **d** = (d_1, d_2) and corresponding values in the transformed coordinate system is obtained by the following in Equation 1.2 (Eriksson and Siska, 2000) :

$$\begin{bmatrix} d'_1 \\ d'_2 \end{bmatrix} = a * R_\alpha * \mathbf{d} = \begin{bmatrix} \frac{1}{a_{max}} & 0 \\ 0 & \frac{1}{a_{min}} \end{bmatrix} \begin{bmatrix} cos\alpha & -sin\alpha \\ sin\alpha & cos\alpha \end{bmatrix} \begin{bmatrix} d_1 \\ d_2 \end{bmatrix} \tag{1.2}$$

In 3D anisotropy is parameterized by strike (α), dip (β) and plunge (ϕ) angles and ratios r_1 defined by minor and major directions, and r_2 is the ratio of vertical and major ranges. The extension

from 2D to 3D is straightforward:

$$d^2 = \begin{bmatrix} d_1 & d_2 & d_3 \end{bmatrix} R_o^T R_o \begin{bmatrix} d_1 \\ d_2 \\ d_3 \end{bmatrix} \tag{1.3}$$

where, $R_o = R_\phi R_\beta R_\alpha$ is combined rotation sequence of the three angles

$$R_o = \begin{bmatrix} cos\alpha cos\phi - sin\alpha sin\beta sin\phi & -sin\alpha cos\phi - cos\alpha sin\beta sin\phi & cos\beta sin\phi \\ \frac{1}{r_1} sin\alpha cos\beta & \frac{1}{r_1} cos\alpha cos\beta & \frac{1}{r_1} sin\beta \\ \frac{1}{r_2}(-cos\alpha sin\phi - sin\alpha sin\beta sin\phi) & \frac{1}{r_2}(sin\alpha sin\phi - cos\alpha sin\beta cos\phi) & \frac{1}{r_2} cos\beta cos\phi \end{bmatrix} \tag{1.4}$$

The calculation of the anisotropic distance between two locations separated by d is achieved by coordinate transformation using local rotation matrix (Equation 1.2 and 1.3).

1.2 Motivation for LVA Fields

There has been interest in utilizing LVA fields for geostatistical estimation. Several methodologies exist which show that when modeling complex, undulating structures accuracy is increased by incorporating LVA fields. By comparison, traditional methods such as kriging gives disappointing results and this problem can be easily shown through a small 2D example of an anticlinal feature (Figure 1.3). Synthetic drill hole data are taken from the outcrop data at two locations as input. The associated LVA is generated with a moving window technique that parameterizes the local heterogeneities and the orientation lines follows the natural anticlinal pattern. It becomes apparent (Figure 1.4) that the original geometry of the bedding cannot be clearly reproduced by standard kriging as any single direction of anisotropy is not sufficient to capture the underlying geologic continuity present in the domain. This example illustrates the idea that variables of interest such as the distribution of mineralized gold veins, or porosity and permeability values in a porous rock media often show LVA. So a quantitative representation of anisotropy in the form of an LVA field must be considered in modeling nonstationary deposits.

While it is rare to find a deposit that is truly isotropic, complex LVA are widespread in geology. Meandering continuity paths seen in fluvial reservoirs are particularly hard to model with pixel based techniques. In order to produce correct flow path response, the spatial pattern and general connectedness has to be maintained. In Figure 1.4 it is shown that continuity is preserved through estimation with LVA because information on spatial distribution of a variable cannot be fully discerned from limited data. The next example further builds upon the case for considering LVA. A 2D section from a meandering channel (Hassanpour, 2013) model is taken in Figure 1.5 and an LVA field is generated as a crucial step prior to assaying the sample data.

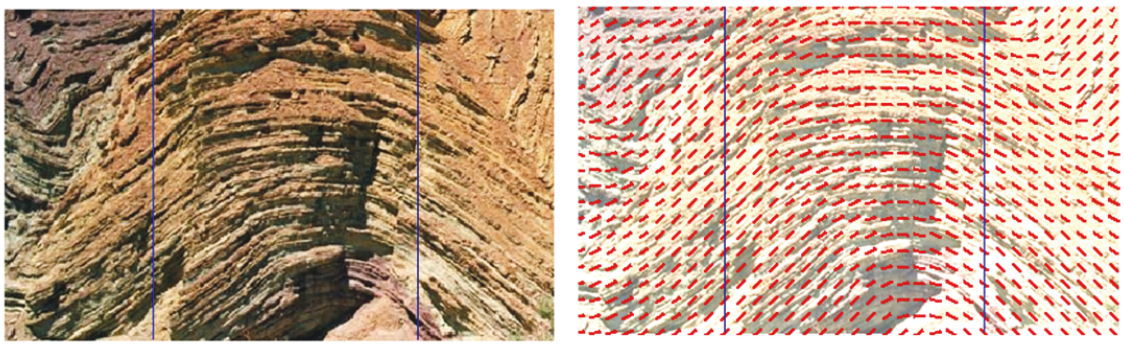

Figure 1.3: A 2d anticline bedding is used for generating synthetic drill hole data at two location (solid blue lines). (Right) LVA field for the analog. The plot dimenstion is 400×241 units. (Source : http://geology.about.com/library/bl/images/blanticline.htm)

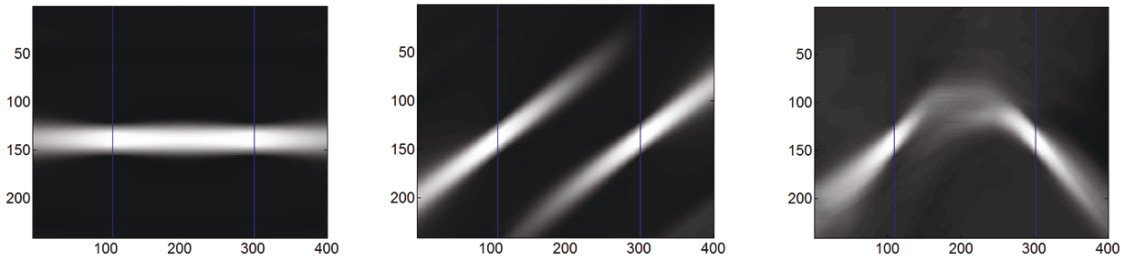

Figure 1.4: (Left and middle) Estimation with kriging considering a horizontal and 60° anisotropy. (Right) Kriging with LVA is used to assay the drill hole data and the plot suggests anticlinal spatial structure.

The consideration behind LVA field is to have a parametric representation of complex geology derived either from available data or an associated exhaustive secondary variable. If samples are sparse, LVA field can be constructed from additional knowledge and imposed in numerical modeling in kriging or simulation. In many depositions the assumption of a constant anisotropy is inappropriate and to circumvent the issue, practitioners subdivide the domain and model stationary areas separately. The process is tedious, inefficient and can result in discontinuous regions that are not consistent as a whole. Classical geostatistical methods are being modified to introduce non-stationarity into modeling but often these require a parametric map of local continuity and magnitude. There are limited techniques available to infer an LVA field and availability of direct angle measurements are sparse.

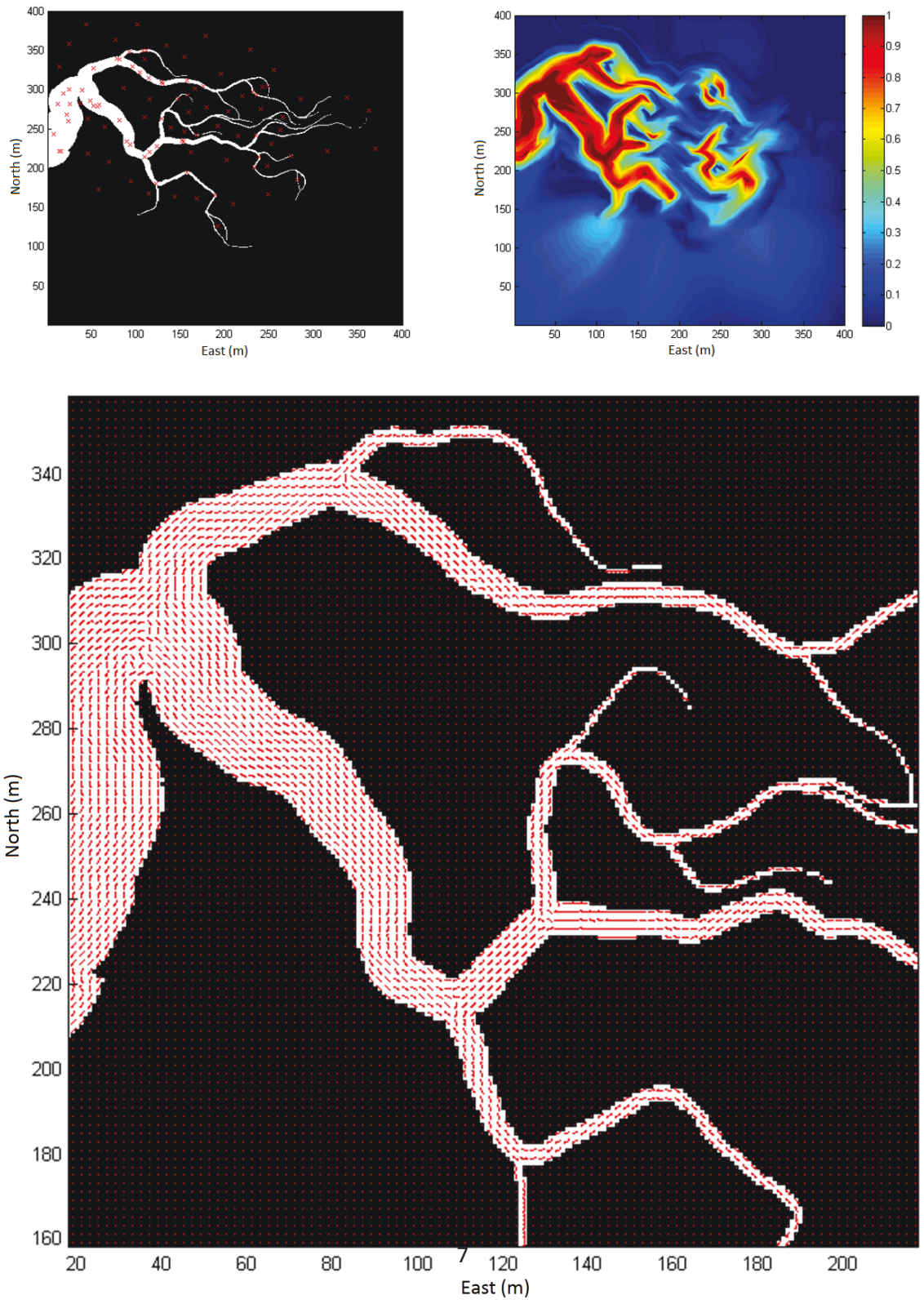

Figure 1.5: A 2D case for modeling a meandering channel cross section (Hassanpour, 2013) motivates the need for considering LVA. Data points are randomly selected by hand (top, left) for non-stationary kriging. The LVA field is generated by keeping in mind the anisotropy here varies with scale.

1.3 Overview of Fundamental Concepts

The key aspect of geostatistical interpolation is to extract spatial patterns of regionalized variables. If there are n observations of a property in a region D the sample data values are defined by {$z(\mathbf{u})$, ($\mathbf{u}$)=1, ... n}. This data set can be thought of as a small section that belongs to a larger set of objects and as such an infinitely many observations are possible in that region. The sample value $z(\mathbf{u})$ represents one outcome from some random process. Formally, the spatial random mechanism that gives the measured value at a particular location is called a random variable (RV) denoted $Z(\mathbf{u})$, and $z(\mathbf{u})$ represents a realization from the spatially regionalized RV (Wackernagel, 1998). A random variable can represent both discrete (rock facies or soil type) and continuous values (mineral ore grade, porosity etc) in the modeling space.

When predicting at an unsampled location ($\mathbf{u_0}$) it is desirable to not only have an estimate but also a measure of uncertainty associated to it, as usually interpolation is based on limited data. Generally a few sampled data does not have sufficient geological information on the actual spatial distribution of the property at hand. In order to quantify the level of uncertainties a probability distribution is determined at each unsampled location. This approach yields a set of possible values attached to a probability distribution function where each outcome or estimate has a corresponding level of uncertainty. For instance estimating copper grade at unknown ($\mathbf{u_0}$) the possible realizations are given by:

$$P(Z(\mathbf{u}_0) < z) = F_{\mathbf{u}_0}(z) \tag{1.5}$$

An assumption of stationarity has to be made prior to any estimation. Stationarity is the decision on how to pool all the data in the domain so that a global mean can be calculated by assuming the regionalized values come from a single population. This is first order stationarity and there are established practices to using locally varying means (McLennan, 2008). Second order stationarity defined through the covariance function suggests $C(\mathbf{h})$ between a fixed set of points is translation invariant. This means for any two points in a domain separated by a lag $\mathbf{h}$, the covariance function is constant for the whole region. This assumption of second order stationarity is not straightforward to deal with and maybe considered inappropriate for modeling complex formations. Refer back to the model in Figure 1.5 it is clear that the 2D section of the meandering deposit is non-stationary. To bring realism into geostatistical modeling this second order non-stationarity can be introduced through LVA field.

$$C(\mathbf{h}) = E[Z(\mathbf{u}) \cdot Z(\mathbf{u+h})] - m^2 \tag{1.6}$$

The covariance function (Equation 1.6) is a measure of spatial variability and is usually calculated from a variogram (γ) function. So for a stationary mean and variance in the region the covariance is calculated as:

$$\gamma(\mathbf{h}) = 1/2\{E[Z(\mathbf{u}) - Z(\mathbf{u+h})]^2\} = C(0) - C(\mathbf{h}) \tag{1.7}$$

$$C(\mathbf{h}) = \sigma^2 - \gamma(\mathbf{h}) \tag{1.8}$$

1.4 Problem Setting

For many deposits in the mining and petroleum industry it is inappropriate to assume second order stationarity for the modeling domain. One way of incorporating non - stationarity into modeling is to consider techniques that incorporate LVA fields. Traditional kriging can be considered when the change in anisotropy is very gradual, i.e. locally the anisotropy orientations are all smooth and consistent and any change in the direction of continuity occurs over great distances. However, modeling of fluvial channels or other complex structures e.g. crossbedding, are more difficult with standard techniques that can only handle a single direction of anisotropy. Building an accurate geostatistical model has implications for subsequent reserve volume calculation, prediction of the flow path in reservoirs etc that are important considerations in the industry.

Many works have been aimed at incorporating these type of heterogeneities into geostatistical modeling since it is clear that the assumption of second order stationary is inappropriate for many deposits. The techniques address the problem by relaxing the stationarity requirements of traditional geostatistics. These techniques often require a continuity field or a LVA field of the underlying structures. The LVA field need not be interpreted from direct samples but additional information from geologic surveys, outcrop data, geologic knowledge of the deposit can also be a source of data for generating an exhaustive LVA field. It should be kept in mind that LVA field inference is domain and data specific, treatment of every deposit is unique as the geology, scale, sample data type, etc will vary. This dissertation presents specific methodologies for the inference of LVA fields from three different data sources typically available: (1) 3D point data; (3) exhaustive data and (3) geological compact bodies.

Next, existing techniques for incorporating LVA in models are reviewed. While this work is focused on generating the LVA field it is important to mention how it would be incorporated into geostatistical modeling.

Boisvert (2010) uses the LVA field to trace the shortest path using a non Euclidean distance metric. Typically anisotropic distance between two locations is calculated by the given anisotropy

orientation of the axis system and the magnitude of the anisotropy. Contrary to the conventional method, in Boisvert (2010) the distances are calculated such that the anisotropy orientation, obtained from an exhaustive LVA field, may be different for each grid node. Locations related about a path that have that smallest anisotropic distance are related in the direction of anisotropy. This distance formalism is incorporated into kriging and sequential Gaussian simulation (SGS), and subsequently estimation nodes along the shortest path receive a higher kriging weight.

Several other kriging variants exist in literature that also requires an LVA field as input, often the anisotropy at each location to be estimated is reoriented through local search (Deutsch and Lewis, 1992; Sullivan et al. 2007 and Xu, 1996). If the conditioning data is dense enough that non stationary features are easily recognizable, then this technique often works well. When estimating a property value at each node the variogram structure is aligned to the local orientation, i.e. the orientation at the estimating location is applied to the search neighbourhood. If LVA changes on a scale smaller than the data spacing Boisvert (2010) is preferred.

Local anisotropy kriging (LAK) developed by Stroet and Snepvangers (2005) automatically determines the local anisotropy orientation through an iterative image analysis method. However the conditioning data must be dense enough to show the non-stationary features of interest (De Jager, 2012). In case the LVA is not apparent, owing to sparse data, this iterative technique cannot capture the heterogeneity of smaller features. Also, the technique may have limited application as it is currently available for only 2D cases.

Apart from kriging based applications, non-stationarity can also be considered through multiple point statistics (MPS) (Strebelle, 2002; Arpat and Caers, 2007). These methods are suitable for reproducing complex rock facies structures and rely on stationary training images (TI) for input on underlying curvilinearity. The TI essentially stores information on geological patterns. MPS algorithms rely on these training images to generate a model (often mostly categorical variables such as facies types) by extracting non-linear features from the TI. Although traditionally stationary TIs are utilized there has been interest for incorporating LVA for the generation of non-stationary TI as a more extensive set of realizations are possible from a single TI by affinity transformation of the local search patterns (Caers and Zhang,2002; Strebelle and Zhang, 2005). An exhaustive LVA field is needed where the anisotropy orientations impose the range for the data transformations.

1.5 Thesis Outline

This work is concerned with obtaining an LVA field that allows non-stationary conditions to be used in geostatistical algorithms. Several techniques are explored for LVA field generation from mapped

or exhaustive data, axial data in the form of point orientation measurements and centerlines of complex objects from geological bodies. In Chapter 2 a preprocessing technique aimed at 3D directional data is discussed. This method however, does not allow for plunges angle consideration. A different approach is taken so that all three angles that determine anisotropy orientation can be used when necessary.

In Chapter 3, LVA orientation is obtained from exhaustive data by calculating the orientation of local windows; a technique is presented to optimize the window size to obtain better LVA definition for cases where anisotropy varies at different scales. Evaluation of centerline extraction from geologic bodies is also presented.

Typically it is necessary to combine information from separate LVA fields and in Chapter 4 a tensor based method is considered to generate a single LVA field. Apart from merging several LVA sources, orientations may also need to be smoothed so that anisotropy follows a logical progression in the exhaustive LVA field map. Chapter 5 presents a case study for inferring LVA field for a copper porphyry mine by fitting manual polylines to each XY layer which are interpolated down to the end of vertical domain. Traditional kriging and kriging with LVA are applied for predicting mine geology and practical issued addressed.

Chapter 2

LVA field generation from Point Data

2.1 Background

It is possible to have direct angle measurements of the variable of interest. This type of data is usually a description of local anisotropy properties. In 3D the orientation is often reported as strike and dip angles and serves as direct measurement of the LVA field. Geologic properties can be inferred directly from strike and dip angles. The strike angle (α) measured from positive north in the horizontal plane refers to the direction of maximum continuity; dip(β) is the acute angle at the intersection of the bedding plane and the horizontal. In Figure 2.1 strike and dip angles describe the orientation of the inclined plane with respect to the horizontal. These angular data are taken relative to a coordinate system where 0° is due north and angle measured clockwise from North is positive and describes how a plane is oriented in space.

Often a third angle is needed to describe the geology completely where plunge (ϕ) is the angle between the horizontal plane and the inclined linear structure in the vertical plane. While concept of plunge is needed for modeling specific geology such as the plunging limbs in a syncline (Deutsch and Journel, 1998), the planar orientation of many structures are defined adequately by strike and dip measurements.

In geostatistics anisotropy is specified by orientation of a coordinate system and associated magnitudes to each direction. Coordinate transformations used here follow the GSLIB convention (Deutsch and Journel,1998) which allows the re-oriented axes to align along the true anisotropy. The variable of interest is then isotropic in this space and has two important advantages: (1) true anisotropy orientation can be captured in the modeling process and (2) it serves as a geological underpinning as the anisotropy is realized through a single matrix (see Equation 1.4). In standard coordinate system positive X lies in the Easterly direction, Y axis is oriented along north direction

(describes the maximum direction of continuity) and Z axis is the upwards vertical direction, and this original system is rotated along strike, dip and plunge so that the orientation of the geological structure is accounted for.

The first rotation is the sequence of transformations is a strike (α) rotation about the Z axis, that rotates the Y axis clockwise from positive North (Figure 2.2). The next step is a rotation of the Z axis and intermediate Y' axis and makes the Y' axis dip from the horizontal plane by dip angle (β) taken negative relative to the initial XY plane. The final rotation is about Y'' axis whose orientation is fixed by the strike and dip rotations. Remaining X', Z' axes turn clockwise about the new principal direction (clockwise when looking down towards the origin) by plunge angle (ϕ). The anisotropy angles referred in this thesis complies with this GSLIB standard (Deutsch and Journel,1998).

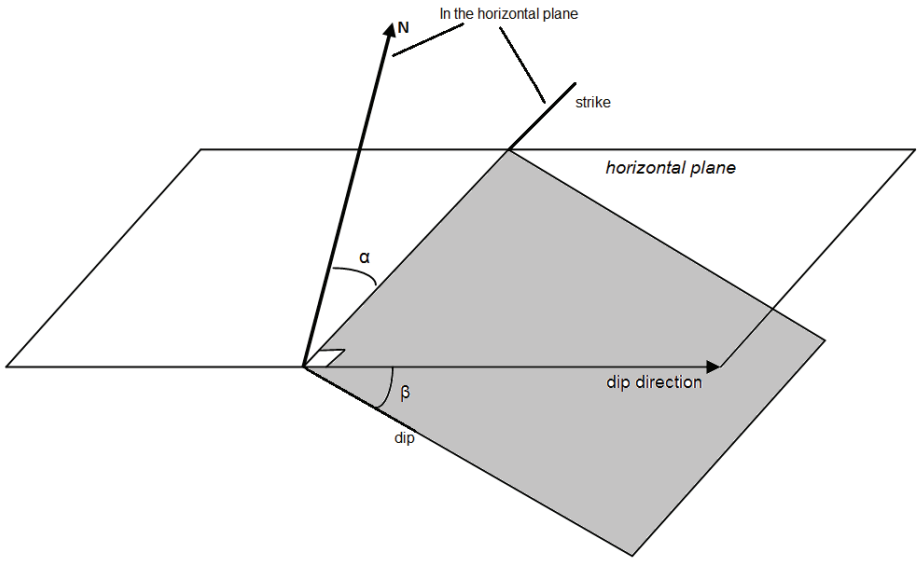

Figure 2.1: A 3D perspective diagram showing strike and dip of the grey plane. Strike and dip direction are horizontal azimuth and lie on the same plane. Dip angle is the inclination of the plane below the horizontal. (After Allmendinger et al, 2012, Fig.1.1)

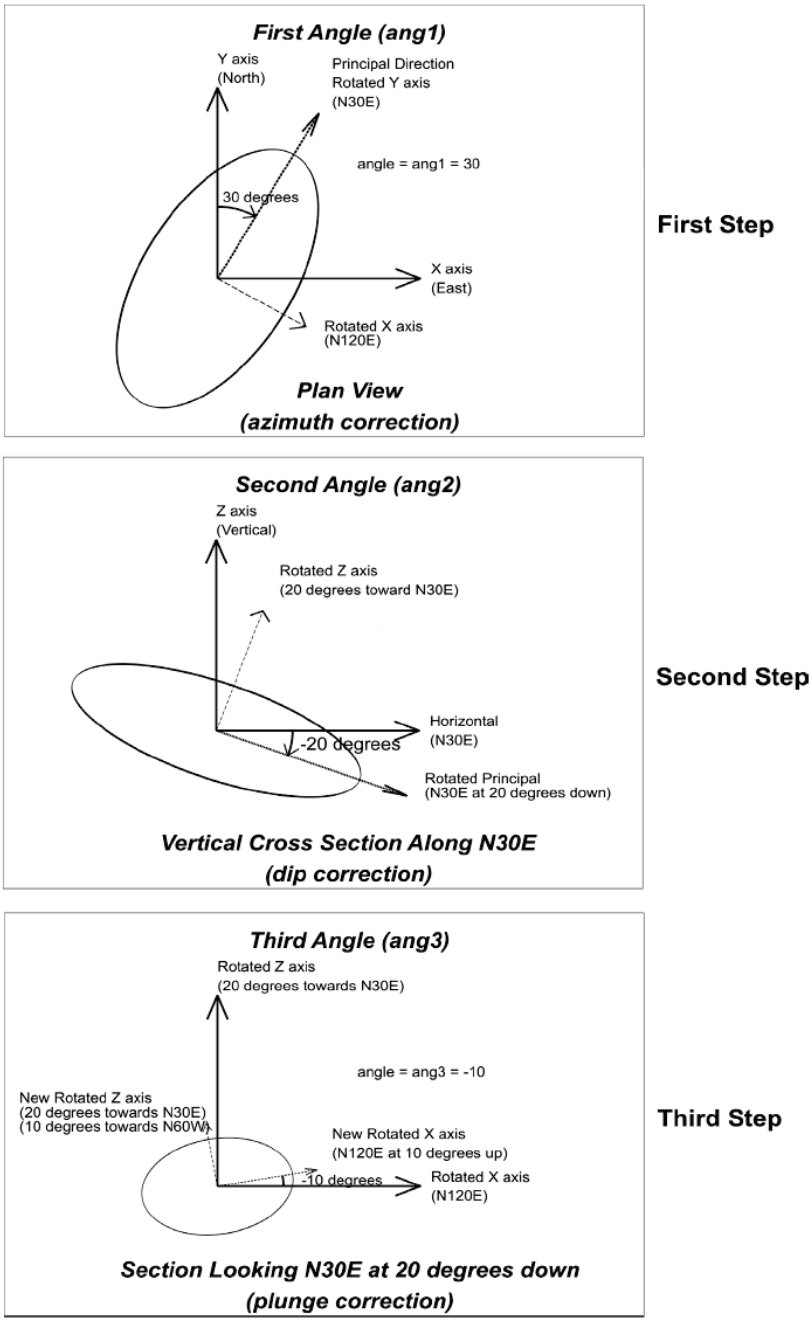

Figure 2.2: Illustration of angle rotations following GSLIB convention. (Original Source : Deutsch and Journel,1998; Reprinted : Neufeld and Deutsch, 2004)

Direct angle measurements can be found from outcrop analogs, exposed underground rocks, bore hole cameras. Formation dip can also be inferred from FMI data, and dipmeter measurements (Boisvert, 2010). Typically data sampling is done at limited locations and only information on local orientation is obtained. Point samples are a special case of directional data known as axial or undirected data where a strike of x is indistinguishable from $x + \pi$ i.e. only the axis of the orientation is important. The surface faults in geo-data is an example of 3D axial data where there is an axis of orientation but no direction (positive or negative axis) (Schuenemeyer and Drew, 2011). Point data can be used in generating an LVA map, but requires unique preprocessing so that the axial nature of the orientation can be captured. The treatment of 2D axial data described in Mardia and Jupp (2000), involves limiting the data to π, then doubling the angles before decomposing into circular components. Standard estimation techniques such as kriging and inverse distance can then be applied to the components to interpolate an exhaustive LVA field.

3D point data on the other hand requires a different treatment. Much like in 2D data, representing bipolar axes cannot be directly modeled for estimation as angles are continuous which presents some unique challenges during estimation. Spherical statistics is used to deal with axial data and the theory is similar to techniques in circular statistics. The next section discusses how the axial nature of the data is preserved before an LVA field is generated.

2.2 Treatment of 3D axial data

Directional data in three dimensions are observed when measuring the magnetism in rocks, optical axes in quartz crystals and geologic faults. Data measuring the orientation axis can be represented as points in a unit sphere (Mardia and Jupp, 2000). Typically point samples from direct angle measurements have strike and dip. Although three angles (strike, dip, and plunge) are considered in 3D to fully describe the anisotropy, plunge is often zero.

The data points are continuous i.e. $360^\circ = 0^\circ$, the point data needs unique treatment before estimation at unknown locations (Boisvert, 2010). Consider the results when inference is carried out directly from available data of two point measurements (Figure 2.3, top). Data points lie in the positive (X) and negative $(-X)$ axes of the same pole or axis of orientation. Each input is defined by strike and dip and is decomposed into spherical polar coordinates. The direction X is decomposed as:

$$X(x, y, z) = (sin\alpha cos\beta, cos\alpha cos\beta, sin\beta) \tag{2.1}$$

The LVA field after applying kriging is unreliable as orientations are inconsistent with orienta-

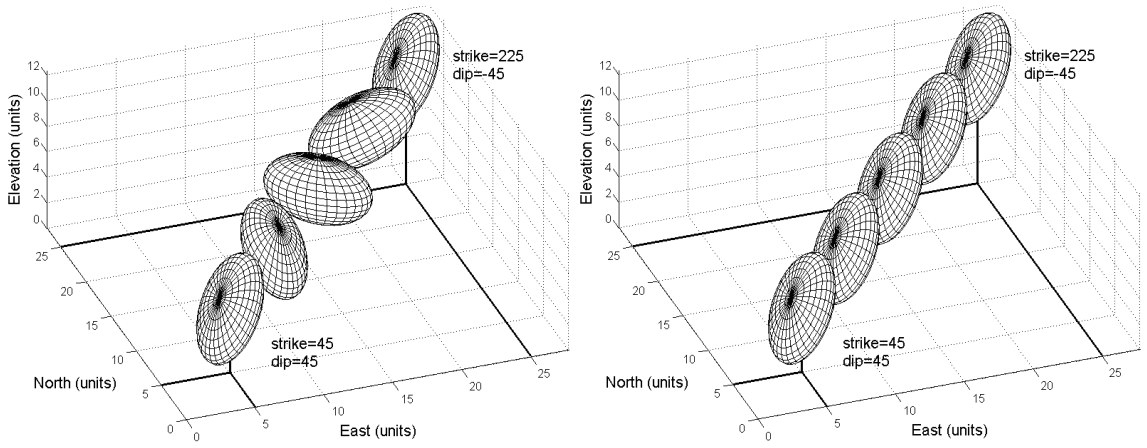

Figure 2.3: Two data points are considered such that they point in opposite direction in the same axis i.e. antipodal pairs. (Left) Without preprocessing the input the axial nature of the point data is not considered in kriging. (Right) The logical change in LVA directions between the two points should lie on the axis of orientation and that is captured. Estimation here is done by considering the nearby combination of point data that has the smallest spherical angle variance.

tion angles ranging between the two initial angular data. Input data therefore must be preprocessed so that axial nature of data is recognized by any interpolation technique (Figure 2.3, right). Estimation techniques like kriging would treat strike 45° and 225° as opposite, when really they lie in the same axis and are continuous. So there is a need to configure which orientations (positive or negative axis) in the sampled points give the best estimate at any unknown location.

2.2.1 Descriptive Statistics for 3D axial data

Unlike in 2D, the 'doubling' of angles is not a sufficient measure to capture the true axial characteristics in 3D. Instead the data can be described as points in a sphere in S^3 and then quantify the dispersion of the points. Descriptive statistics, such as variance of a set of angles, provides a good measure in choosing axial orientations. For any number of sampled points our aim is to (i) align data on the same axis or along axes with small deviation and (ii) provide continuity of features among the known points and estimate. The spherical variance (σ^2_{sp}) measures how spread out the data is in space. If the points are aligned pointing largely in the same direction, about similar axis of orientation then σ^2_{sp} is small. Generally, an estimate using a cloud of points with the minimum attainable σ^2_{sp} would be a good approximation of surrounding orientations. It is important to distinguish between this spherical angle variance (σ^2_{sp}) and kriging variance used in interpolation.

Angle variance helps in selecting an angular configuration such that the estimate is smooth and logical. For any number of conditioning data, the aim is to determine the combination of data that results in the minimum variance of the angles. Consider a set of orientations represented as unit vectors x_1 … x_n on S^3, the sample mean orientation is:

$$\bar{x} = \frac{1}{n} \sum x_i \tag{2.2}$$

The sample spherical variance is calculated as:

$$2(1 - ||\bar{x}||) = \sigma_{sp}^2 \tag{2.3}$$

This spherical variance is computed for all combinations of orientations for the surrounding conditioning data found within the estimation search window.

2.2.2 Kriging with point data

Consider three sample points being used to estimate at an unknown location (Figure 2.4). The proposed technique is to determine which axial orientation would be consistent for all three locations. There are a total of 3 different situations and the variance of the angle data can be used to determine which of the three orientations should be averaged. Since, there are three locations, consider flipping one location at a time and recording the associated spherical angle variance. As indicated on Figure 2.4, the combination where location u_3 is 'flipped' (consider the opposite axis) has the minimum variance (Table 2.1). A value of '0' de s an original orientation and a '1' indicates the flipped or the opposite orientation.

The sample at location u_3 should be rotated to point in a similar direction as the other data; this is reflected in the minimum variance of the angles. More combinations are required for considering a larger number of conditioning data, but flipping one orientation at a time and passing through the conditioning data once is sufficient to find the optimal number of flips; this process is not computationally demanding. The combination with the minimum variance is selected and traditional estimation of the components of x is implemented. The methodology is implemented on a synthetic 3D axial data (Figure 2.5) and component-wise decompositions for the domain of interest are shown (Figure 2.6). LVA field (Figure 2.7) is generated by recombining the estimated components.

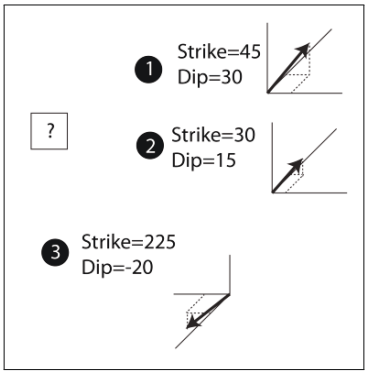

Figure 2.4: Estimating at an unsampled location (?) from three conditioning data at locations u1,u2 and u3.

Table 2.1: Angle variance for all combinations of input data shown in Figure 2.4. '1' indicates the orientation has been flipped.

u_1	u_2	u_3	Variance
0	0	0	0.60
1	0	0	0.60
0	1	0	0.58
0	0	1	0.01

2.3 Incorporating Plunge

The benefit of considering the flipping of the angles is that any geostatistical estimation methodology could be applied to generate the exhaustive LVA field. The drawback is that a plunge angle cannot be considered. In the rare cases where a plunge angle is required, the orientation of point data can be defined using a quaternion. They are 4-tuple entities are routinely applied in determining attitudes for instance of spacecrafts by combining data from several attitude sensors. Quaternions representation is based on the well known Euler's rotational theorem that the relative position of any two arbitrary, rigid coordinate systems can be represented by a single rotation about a fixed axis (Grobekatthofer and Yoon, 2012). The fixed axis or rotation axis is u, and the single rotation angle is denoted θ (Figure 2.8). A quaternion can be defined as a vector

$$q =< q_0, q_1, q_2, q_3 >^T$$

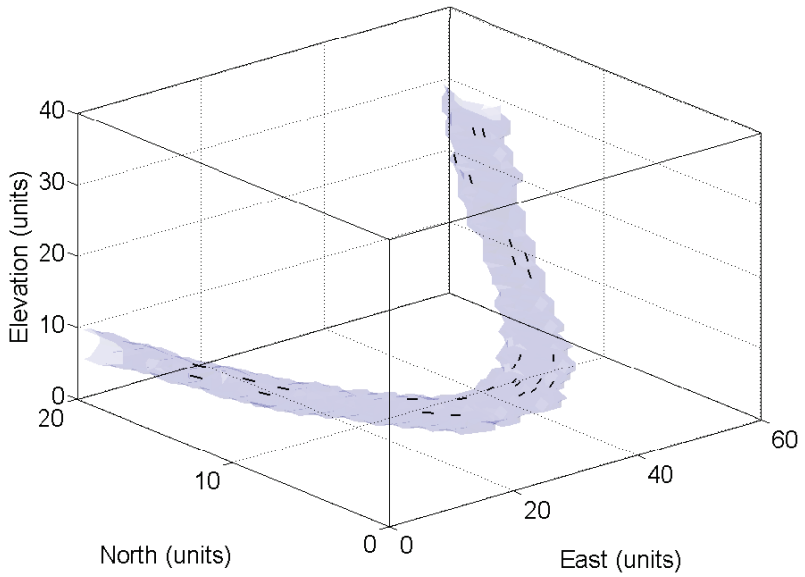

Figure 2.5: The shaded represent the shape of the underlying syncline model; at discrete locations the orientations are taken as synthetic angle data and are represented by the orientation lines.

By convention entities used for parameterizing attitudes are unit quaternions, whose components all have absolute value of less than or equal to 1.

The elements q_1, q_2, q_3 comprise the vector part of the quaternion, which is imagined as the axis of rotation. q_0 is a scalar that defines how much rotation is performed about the rotation axis given an angle of rotation (θ). To define the Euler rotation angle $R_{q,\theta}$ with a quaternion , we define first the terms q_0 and $(q_1, q_2, q_3)^T$ as:

$$< q_0, q_1, q_2, q_3 >^T = < cos(\frac{\theta}{2}), \overrightarrow{e} sin(\frac{\theta}{2}) >^T \tag{2.4}$$

For a normalized quaternion $\overrightarrow{e}$ is the unit length rotational axis and θ is the rotational angle (Yang, 2012). For spatial interpolation direct angle measurements need to be transformed into quaternions as the first step by equation (2.5). This mapping is particular to the sequence of rotations described in Deutsch and Journel (1998) that define anisotropy direction in 3D.

$$q(\alpha, \beta, \phi) = \begin{bmatrix} cos(\frac{\phi}{2})cos(\frac{\beta}{2})cos(\frac{\alpha}{2}) - sin(\frac{\phi}{2})sin(\frac{\beta}{2})sin(\frac{\alpha}{2}) \\ cos(\frac{\phi}{2})sin(\frac{\beta}{2})cos(\frac{\alpha}{2}) - sin(\frac{\phi}{2})cos(\frac{\beta}{2})sin(\frac{\alpha}{2}) \\ cos(\frac{\phi}{2})sin(\frac{\beta}{2})sin(\frac{\alpha}{2}) + sin(\frac{\phi}{2})cos(\frac{\beta}{2})cos(\frac{\alpha}{2}) \\ cos(\frac{\phi}{2})cos(\frac{\beta}{2})sin(\frac{\alpha}{2}) + sin(\frac{\phi}{2})sin(\frac{\beta}{2})cos(\frac{\alpha}{2}) \end{bmatrix} \tag{2.5}$$

The three rotation angles can easily be converted into its associated quaternion (Equation 2.5) and a simple interpolation technique can be used in estimating at unsampled locations (Markley et al,

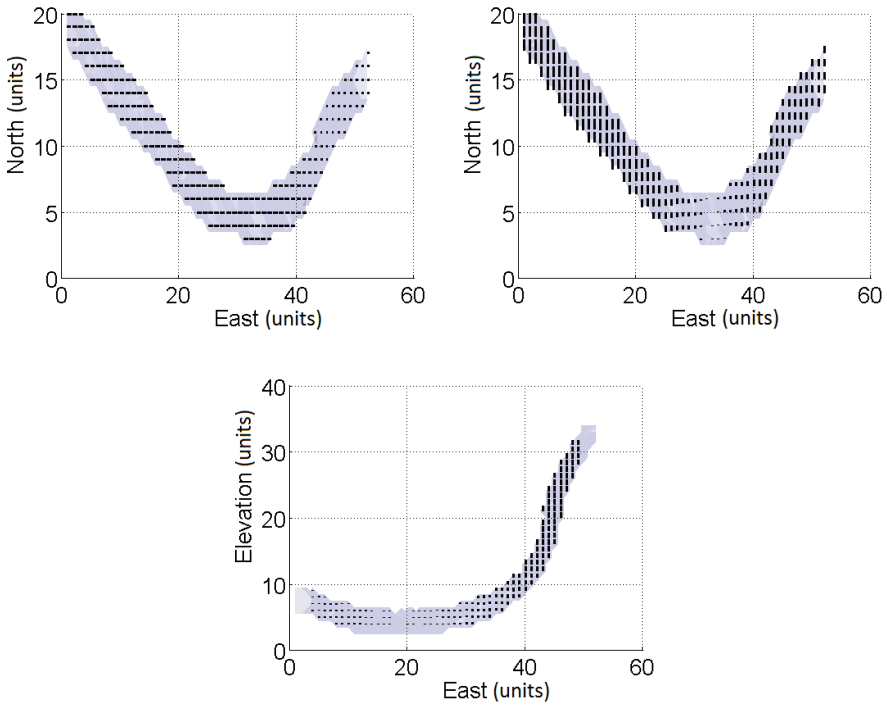

Figure 2.6: Estimation of X, Y and Z components.

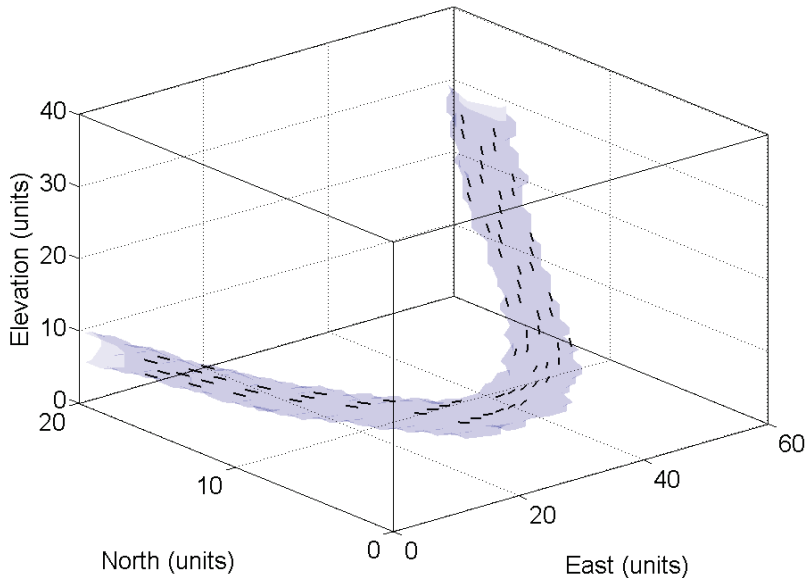

Figure 2.7: The resulting LVA field after preprocessing available data and component-wise kriging.

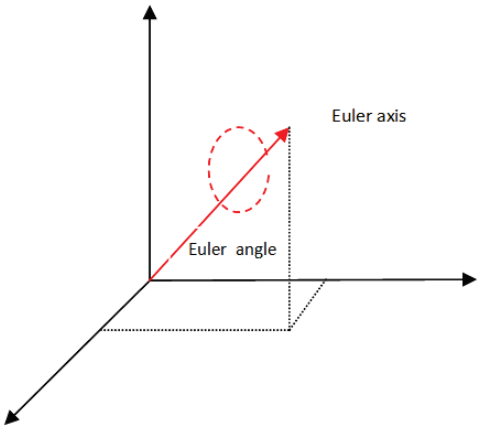

Figure 2.8: A schematic representation of Euler's rotational theorem of a quaternion (After Grobekatthofer and Yoon, 2012, Fig. 9).

2007). The problem reduces to finding a 4×4 matrix M:

$$M = \sum_{i=1}^{n} w_i q_i q_i^T \tag{2.6}$$

where, wi are the local weights determined using the inverse distance method.

The desired average quaternion is the eigenvector of M corresponding to the maximum eigenvalue (Markley et al, 2007). Strike, dip and plunge are found locally by back-transforming the averaged quaternion $(\bar{q})$ by:

$$\begin{bmatrix} \alpha \\ \beta \\ \phi \end{bmatrix} = \begin{bmatrix} atan2(-2q_1q_3 + 2q_0q_2, q_3^2 - q_2^2 - q_1^2 + q_0^2) \\ atan2(2q_2q_3 + 2q_1q_0) \\ atan2(-2q_1q_2 + 2q_0q_3, q_2^2 - q_3^2 - q_0^2 + q_1^2) \end{bmatrix} \tag{2.7}$$

This method can generate a smooth interpolation of the three anisotropy parameters and is shown in Figure 2.9 and Figure 2.10.

2.4 Remarks

Two methodologies for the inference of LVA field from 3D point data is presented here using spherical angle variance method and parameterization of orientation with quaternions. It is often sufficient to describe the geologic structure reporting only strike and dip angles. Working with these

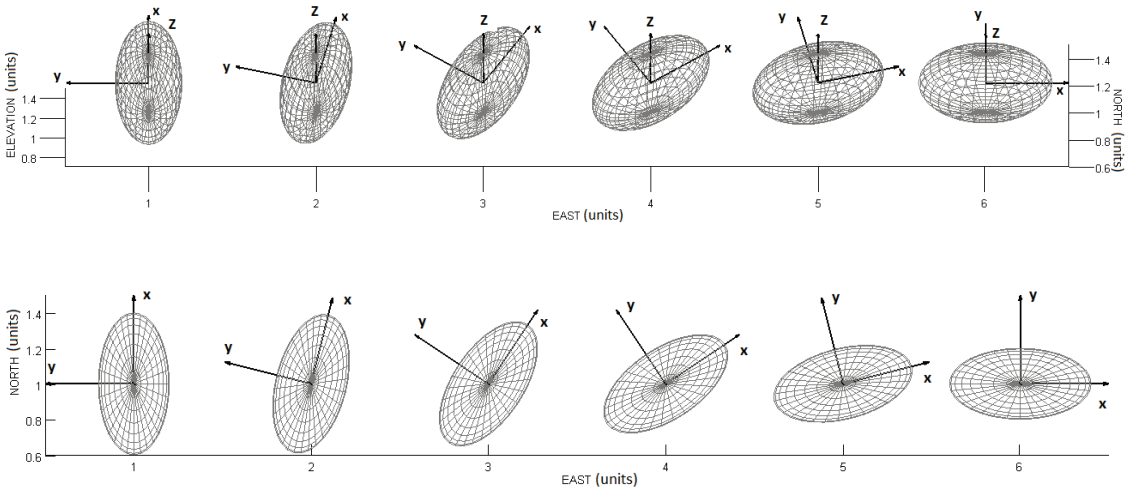

Figure 2.9: A strike of 90° and 0° are given at points x=1,6 (East), y=0 and z=0. The orientations at unknown locations show a smooth change in angles. (Top) 3D view; (Bottom) Plan view along the z-axis.

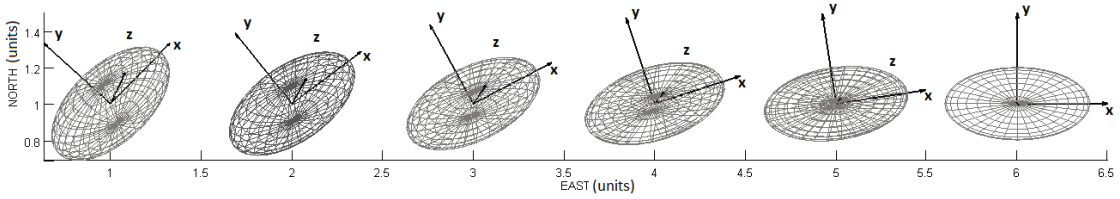

Figure 2.10: Orientations found using averaging quaternion. Point x=1,y=0 and z=0 has a strike = 45°, dip = 20° plunge =10°, and at x=6, y=0 and z=0 angular data are zero. Quaternion averaging produces a smooth LVA estimates using the two conditioning point data.

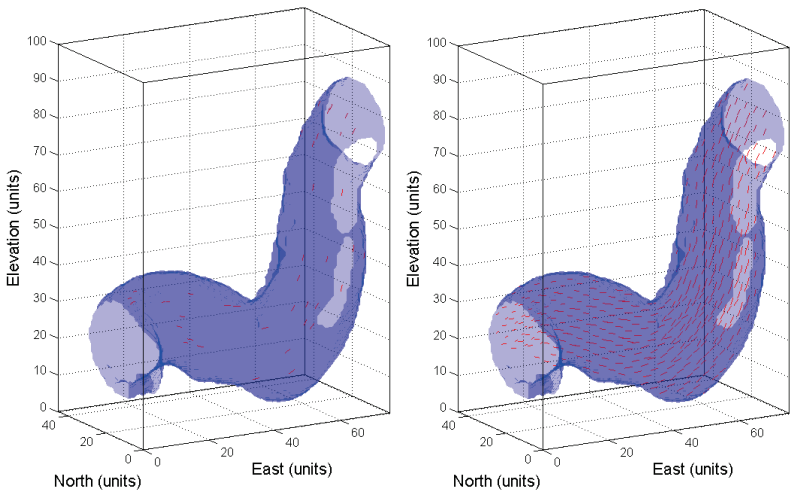

Figure 2.11: A small 3D model used to demonstrate the quaternion averaging result. (Left) Input points taken from a body represented by the shaded part. (Right) Model populated with LVA orientations.

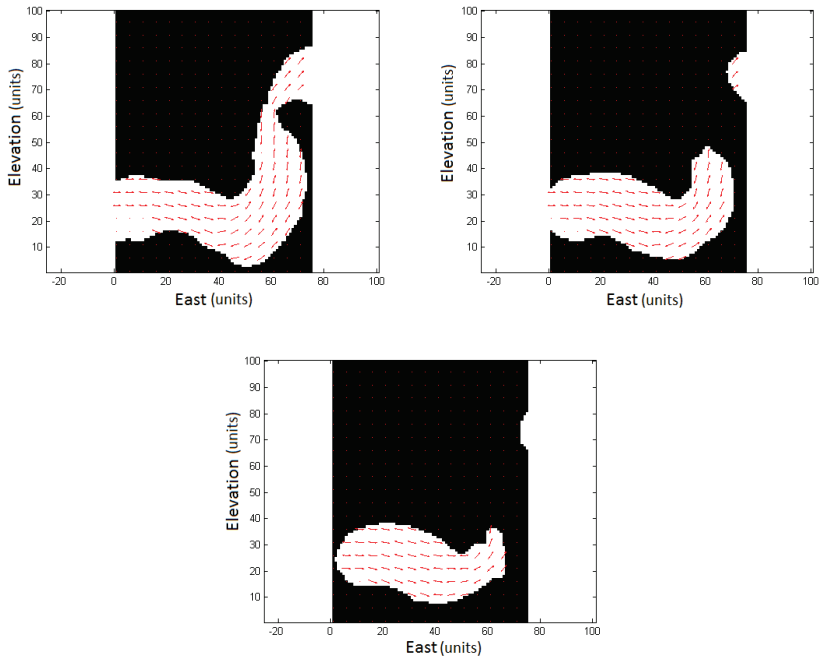

Figure 2.12: Cross sections taken from the 3D model LVA field (above) along North. Slices taken at y=21, 26 and 31.

two angles the anisotropy direction can be easily decomposed into respective components and estimation of an exhaustive LVA field is done by interpolating each component. Local directions are adjusted to have the smallest spherical angle variance. To evaluate at an unsampled location standard kriging is used to build a smoothly interpolated field of local orientations. In specific instances the plunge angle maybe needed to completely parameterize the anisotropy. Then the methodology of reorienting point data cannot be applied as the data described by 3 angles is no longer axial. LVA field is generated by quaternion averaging when plunge angles need to be considered. Local directions for the LVA field are reported with the associated 3 angles from equation 2.7.

While quaternions provide a straightforward way to evaluate 3D point data, their scope is limited to estimating with inverse distance. Inverse distance and kriging are both linear estimators that assign weights to the nearby known data locations by different weighting schemes; however estimation by kriging holds several desirable properties. The important difference between the two lies in the fact that kriging aims to minimize the variance of residual errors and the spatial characteristics can be accounted for. When estimating the X, Y and Z components the pattern of spatial continuity can be captured through variograms allowing for simple trend modeling. It is likely that the local kriging estimate of anisotropy is difficult to improve upon and so when evaluating strike and dip angle measurements it is better to infer LVA field estimates through reorienting point data and kriging rather than applying quaternion averaging.

Chapter 3

LVA Inference from Exhaustive data and Centerlines

3.1 Orientation from Exhaustive Data

Geophysical remote sensing data from seismic, electromagnetic, gravitational and other surveys provide low-resolution, bulk property measurements of the domain which are used in determining regional continuities for a variable. If primary variables are not sampled extensively, a correlated secondary variable from exhaustive geophysical survey data can be used instead. Analyzing the intensity changes from exhaustive data (or calculating gradients of gray values in outcrop images) is an important step for extracting the orientation of local structure.

3.1.1 Gradient and PCA based analysis of local orientation

Tensors have a wide range of application in many fields as they are generalizations of vectors in higher dimensions. They are an important tool in image processing for perceiving textures, edge detection from local changes in contours, intensity signals and directions of adjacent patterns. The motivation for such analysis comes from the fact that physical quantities of complex natural phenomenon – stress at a point on rock mass due to internal forces, electrical or thermal conductivity in anisotropic medium, diffusion, etc – cannot be understood by the use of scalars or vectors, they must be formulated as tensors (Cammoun et al, 2009). In a geostatistical setting, a tensor can be used to characterize spatial anisotropy and can be extracted from exhaustive gridded data. This data can come from seismic, magnetic or gravitational surveys, outcrop images, geological interpretations, etc. It is assumed that the measured bulk variable has the desired spatial characteristics and can be used as a proxy for the underlying LVA field of the variable of interest.

The first step in detecting orientations from exhaustive data is the search for local symmetries in the intensity distribution, which is the basis for finding a linear symmetry or local orientation (Haubecker and Jahne, 1996). The term local orientation means that the change in intensity values show a distinct pattern or orientation and this orientation can be shown by a vector in 2D or orientation angle in higher dimensions. Before the formulation of tensors in 2D and 3D, there is a need to discuss how clear dominant directions can be identified and how such a single direction is obtained. First, the gradient field, $g(\boldsymbol{u})$, is calculated from the exhaustive data. The gradient transformation of the image in 2D has two vector components which now contain the information of change in signal intensities (change in colour intensity in case of grey scale outcrop images). The gradient vectors indicate the direction of maximal change in intensity and is normal to the oriented structure. If gradient vectors cannot identify any dominant directions, the feature is assumed isotropic.

Consider a local neighbourhood A around an arbitrary point $\boldsymbol{u_0}$, and a gradient field $\Delta g(\boldsymbol{u})$ for every point $\boldsymbol{u}$ in the domain. The objective is to find a mean vector $a(\boldsymbol{u_0})$ that unifies all the directional vectors of $g(\boldsymbol{u})$ to give a single local orientation that is invariant to a rotation of π. It is important that the mean $a(\boldsymbol{u_0})$ maximize the average angles with respect to all direction vectors, $g(\boldsymbol{u})$, in A (Feng and Milanfar, 2002). A schematic representation of the problem is shown in Figure 3.1. A projection of $g(\boldsymbol{u})$ onto $a(\boldsymbol{u_0})$ or the inner product of the vectors gives a measure of the proximity of the gradient vectors and $a(\boldsymbol{u_0})$. Moreover, since antipodal directions are the same, the absolute value or square of the inner products can be taken. In order to find $a(\boldsymbol{u_0})$ that lies along the feature and in the direction of least change in the intensity field, the problem is formulated as the following minimization problem :

$$\rho(u) = g^T(u)a(\boldsymbol{u_0}) \tag{3.1}$$

$$Q(u) = \int_{A(\boldsymbol{u_0})} \rho^2(\boldsymbol{u})du$$

$$min(Q) = min(\int_{A(\boldsymbol{u_0})} \rho^2(\boldsymbol{u})du) \tag{3.2}$$

It can be shown that the equation (3.2) can be expressed of in terms of a symmetric tensor T and the vector $a(\boldsymbol{u_0})$ (Cyganek and Siebert, 2009).

$$Q = a^T(\boldsymbol{u_0})T(\boldsymbol{u_0})a(\boldsymbol{u_0}) \tag{3.3}$$

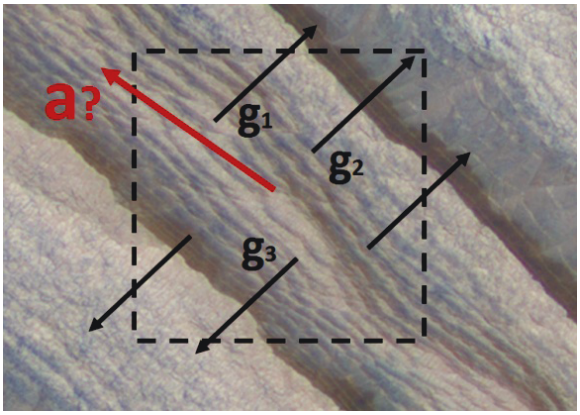

Figure 3.1: The task is to find the orientation of the feature, vector $a(\boldsymbol{u})$, that maximizes the average angles between itself and all other gradient vectors. Gradient vectors (g_i) calculated at different points show local symmetry in the intensity distribution.

where, $T(\boldsymbol{u_0}) = \int_{A(\boldsymbol{u_0})} g(\boldsymbol{u}) g^T(\boldsymbol{u}) du$.

The term T (Equation 3.3) expresses the outer product of the gradient vectors with itself, which is the result of rotation invariance (Cyganek and Siebert, 2009). From equation 3.3 it can be deduced that the minimum is found when $a(\boldsymbol{u_0})$ is the eigenvector corresponding to the smallest eigenvalue of T. This analysis suggests that the task of determining $a(\boldsymbol{u_0})$ is equivalent to eigen-decomposition of the symmetric tensor T, and the dimensionality of T is directly related that of the vector $g(\boldsymbol{u})$ (Cyganek and Siebert, 2009) allowing for similar analysis in higher dimensions. Apart from minimizing the function $Q(\boldsymbol{u})$, the desired mean vector $a(\boldsymbol{u_0})$ can also be formulated as a statistical problem. It involves building a local histogram of orientations (phases of the local gradient vectors) where $a(\boldsymbol{u_0})$ is orthogonal to the gradient vector phase with highest frequency (Lowe, 2001).

Firstly, intensity gradients $\Delta g(\boldsymbol{u})$ are computed from exhaustive data. Then for a local neighbourhood A, about a node $\boldsymbol{u_0}$ the tensor components are:

$$T_{ij}(\boldsymbol{u_0}) = \int A(\boldsymbol{u_0} - \boldsymbol{u}) \Delta g_i(\boldsymbol{u}) \Delta g_j(\boldsymbol{u}) du \tag{3.4}$$

Equation (3.4) is used when the intensity changes are continuous. An equivalent expression for discrete data takes the form:

$$\hat{T}_{ij} = F(D_i D_j) \tag{3.5}$$

D_k is a discrete differentiating operator in the k^{th} axis, and $F(D_i D_j)$ is usually a Gaussian filter used for smoothing. Once the tensors are constructed in two and three dimensions, the next step

is to extract the dominating direction through eigenvalue decomposition. It can be shown that the eigenvectors obtained preserve the invariance to a rotation of π. So, for a given symmetric tensor T the desired orientation of a can be obtained as follows:

$$T = \begin{bmatrix} T_{11} & T_{12} \\ T_{21} & T_{22} \end{bmatrix}$$

$$\vec{a} = \begin{bmatrix} T_{22} - T_{11} \\ 2T_{21} \end{bmatrix} \tag{3.6}$$

There are several ways to obtain this a vector, for instance by rotating T about its principal axis until it aligns with the coordinate axis (Jahne, 1997). Another approach is to perform singular value decomposition (SVD) (Cyganek and Siebert, 2009). Feng and Milanfar (2002) implemented a principal component analysis based feature orientation technique where local orientation is established by performing SVD onto a collection of gradient vectors. A central feature of the technique is to subdivide the gradient field into blocks and perform SVD decomposition on the gradient vectors of each block. In 2D the following matrix is constructed for the individual blocks:

$$G = \begin{bmatrix} \nabla f^T(1) \\ \nabla f^T(2) \\ ... \\ ... \\ \nabla f^T(N) \end{bmatrix} \tag{3.7}$$

where, $\nabla f^T(k) = [\delta f(x_k, y_k)/\delta x, \delta f(x_k, y_k)/\delta y]$ are the gradients at each point k, and G is a N$\times$2 matrix.

The SVD decomposition of the form $G = USV^T$, where U is N$\times$2 matrix with orthogonal columns; S is a diagonal matrix containing the singular values in sorted order; and V is 2$\times$2 orthogonal matrix in which the columns contain information about dominant image orientations. In the geological context this provides the orientation of local features on a map, 3D geological model or exhaustive model.

3.1.2 Basic Workflow

The following steps are used to determine the LVA field orientation in the spatial domain:

1. Calculate the gradients at each point in the model; D_k is the stored gradient value in the k^{th} coordinate direction

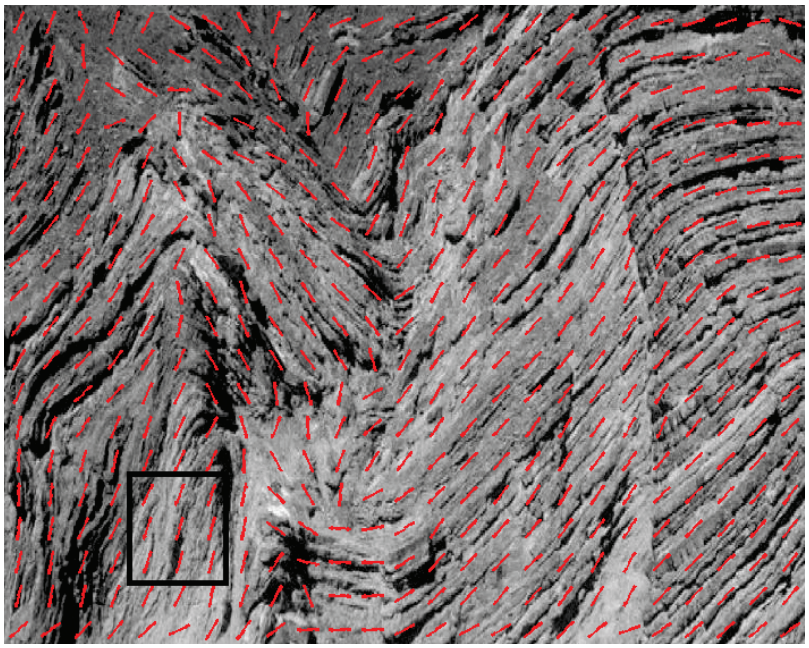

Figure 3.2: Greyscale image of a folded outcrop (Source: http://gsfc.nasa.gov/Sect2/Sect2_1a.html) with the gradient based implementation (arrows) overlain. A window (bottom left) is shown to emphasize that each orientation is obtained from the gradient of a local window. Figure dimensions are 594×780 units.

2. Find necessary products of D_i and D_j for every pixel, and if necessary apply a low pass filter to obtain the components of the tensor matrix T

3. Similarly, a PCA based analysis can be performed with gradient vectors arranged in an N$\times$2 matrix G (Equation 3.7)

   In 2D the tensor matrix for an image location (i,j) is:

$$\hat{T} = \begin{bmatrix} F(D_i, D_i) & F(D_i, D_j) \\ F(D_j, D_i) & F(D_j, D_j) \end{bmatrix}$$

4. Local orientations are obtained from the tensor matrix through eigenvalue decomposition. In the PCA implementation the method is similar with a SVD of matrix G.

The gradient method is applied to the following outcrop image (Figure 3.2) and the associated LVA is generated using the gradient based method. Local orientations are largely consistent with the geologic structures.

3.2 Adaptive Window for Exhaustive Data

3.2.1 Scale of Anisotropy

Different geological systems are characterized by unique combinations of architectural elements that arise from natural processes of weathering, erosion, transportation and subsequent depositions of sediments etc. These physical processes cause properties to be more continuous in one direction and less in another. For example fluvial systems are formed through sedimentation by river currents and are marked by repeated changing of course owing to ground compositions, flow conditions. Anisotropic conditions as a result of deposition and subsequent diagenetic alternations can mature into non stationary features due to the way a deposit is formed. Often these locally varying features show extensive anisotropy at multiple scales varying from pore size to field level (Tiab and Donaldson, 2012; Kopaska-Merkel and Mann, 1992). Consider the deltaic system of Bombetoka Bay in Madagascar (Figure 3.3), it indicates that the style of features vary extensively seen at various scales (Shepherd, 2009).

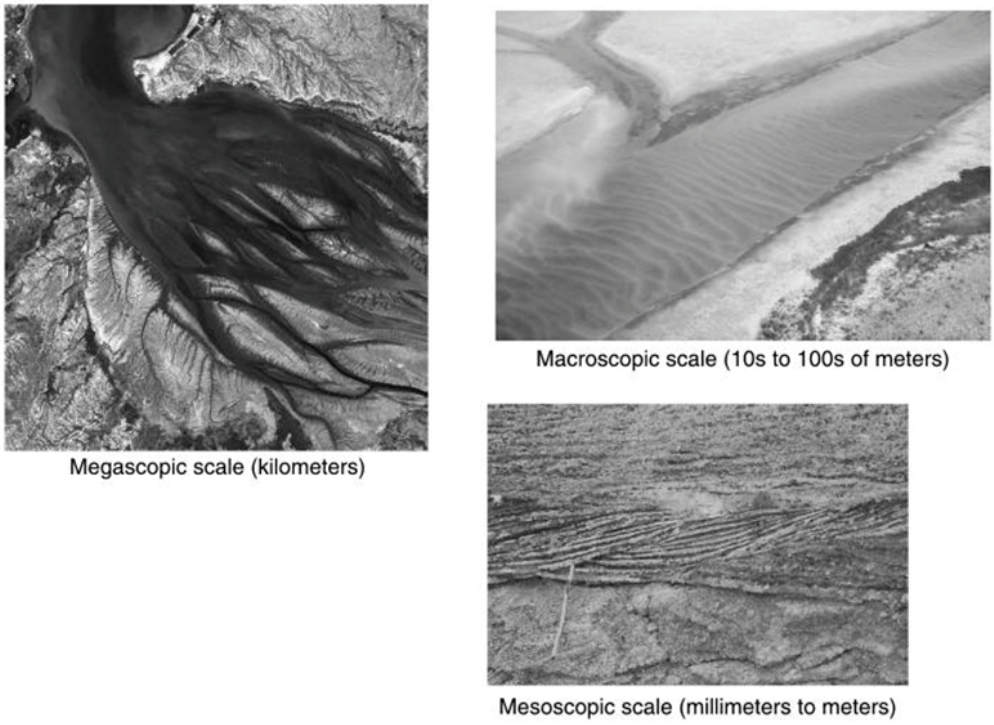

Figure 3.3: Different styles of anisotropy seen at mutiple scales in Bombetoka Bay. Figure considered from Shepherd (2009).

Depositions such as porphyry formations, fluvial, estuarine and magmatic systems can be characterized by different types of styles and scales of heterogeneities. Complex geological interaction occurring at different levels lead to the locally varying features observed over a scale of interest. However, there is some uncertainty as to what features in the deposition should be incorporated into geostatistical model using an LVA field. In geostatistics, conventional models are built on discretized grid cells and a single grid block is the smallest component of the model. Thus the block scale, typically ranging between $5m^3$–10^5m^3, provides the lower bound for the relevant features that are considered for LVA field generation. The end application and computational time will dictate the size of the numerical model, and in essence features larger than the block size and smaller than the modeling domain are deemed pertinent for the assessment of LVA. The user must evaluate the nonstationary features against their impact on subsequent transfer functions and choose the relevant features with the largest impact prior to LVA field generation (Boisvert, 2010). Assessing exhaustive data, that displays non stationary features at different scales, through moving window techniques poses a challenge as estimation so far is done using a fixed window size. A methodology for building the LVA field for such structures is presented in the following section.

3.2.2 Adaptive Window for Exhaustive Data

In the gradient based feature extraction discussed, the nature of the LVA field is largely dependent on the size of the local neighbourhood. Selection of the window size becomes even more relevant when geological deposits display different continuity at different scales. To highlight the problem of choosing an appropriate window size, consider a synthetic example with structures at different scales (Figure 3.4). When a large search area is selected, features of that scale can be effectively captured (Figure 3.4a); however, the appropriateness of this search area is questionable for structures at smaller scales. When scales of geologic continuities differ, orientations at every scale cannot be determined correctly by using a single preset window size (Figure 3.4b). Instead, if the search areas are allowed to vary such that they adapt to the underlying feature scale, a continuous LVA field can be generated that accounts for all apparent features regardless of scale.

The idea of spatially adaptive search window is implemented in Katkovnik et al. (2002) where an intersection of confidence intervals (ICI) rule is used to select an optimal window size or signal bandwidth for filtering image signals. In texture analysis, the use of automated window size selection with a conventional rectangular moving window is based on some threshold criteria. Here, an ellipse is used to define the 'window' or local neighbourhood (an ellipsoid in 3D). For feature detection the methodology enables the window fitted to resemble the underlying scale and the

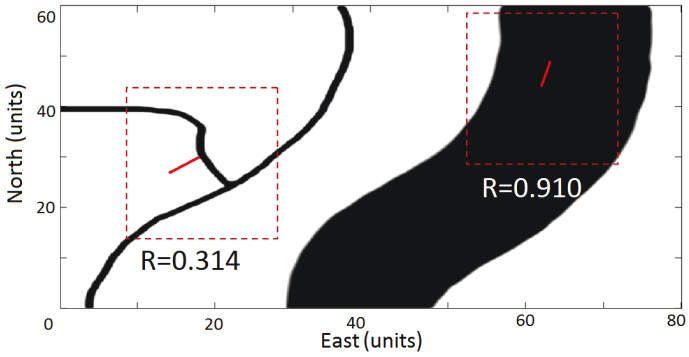

Figure 3.4: (a) A large window size is selected for the domain. While orientations for larger scale features are detected correctly, continuity determined at a finer scale is misleading since there is no single local orientation for that search area. (b) Continuity at larger scale cannot be determined and is considered isotropic since the window size is too small.

direction of anisotropy.

By locally redefining the search windows, the local neighbourhoods can be easily scaled and oriented in a way such that the underlying features are optimally extracted. The parameters of the adaptive window are a rotation angle (θ) and semi major and minor axes lengths. The user selects the ranges of the parameters, the local reliability for every parameter combination is calculated and the largest reliability is selected. The term reliability (R) is a measure of confidence on the estimated orientation and is calculated from the ratio in Equation 3.8 (Jeulin and Moreaud, 2008). Reliability can also be considered a measure of the magnitude of the local anisotropy; however, when implementing geostatistical LVA techniques, the magnitude is often kept constant as the

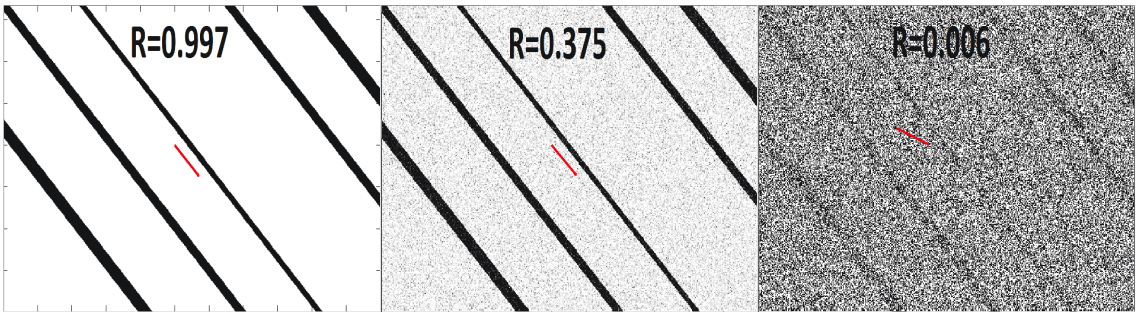

Figure 3.5: Impact of noise on orientation estimation and reliability. Plot dimensions are 500×300 units.

local orientation varies.

$$R = \frac{\lambda_1 - \lambda_2}{\lambda_1 + \lambda_2}, \quad for \quad \lambda_1 > \lambda_2 \tag{3.8}$$

where, $\lambda_{1,2}$ are the two non-zero eigenvalues of the symmetric tensor, T_{ij}.

The value R is bounded between 0 and 1, and is a measure of how dominant one direction of intensity change is compared to another. Figure 3.5 shows estimation of dominant feature direction is robust to low levels of noise even while the reliability drops.

The optimal window selection process is a search over all parameter combinations to find the ellipsoid with the highest reliability measure. This process is done for every local window defined by the modeling grid. Calculation of all parameter combinations at each location may be computationally excessive for large grids. Instead a partial-optimization is implemented where a smaller range of parameters are searched thus decreasing the run-time. The results from the partial-optimization are a good approximation and produces LVA fields that are consistent with the scale of the geology (Figure 3.6). The steps involved in the adaptive window selection are:

1. Consider the exhaustive set parameters in choosing the local window for first grid node and then calculate local orientation
2. Store the combination that gives the highest reliability
3. Use the known parameter values as the base case and consider small ranges from the base case for adjacent cells
4. Optimize the local neighbourhood based on reliability and update the base case

The results are illustrated in Figure 3.6 on a geological body having features at varying scales. When considering the small window size only (Figure 3.6a) the orientations inside the larger features are

modeled incorrectly. When considering the large window size only (Figure 3.6b) the small scale features are not reproduced well. Figure 3.7 is a schematic representation of how the search areas varied throughout the nodes.

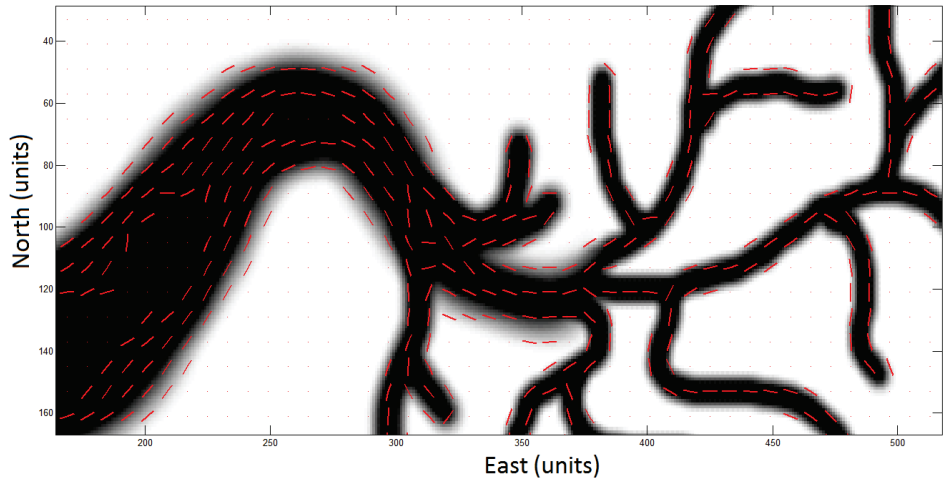

(a)

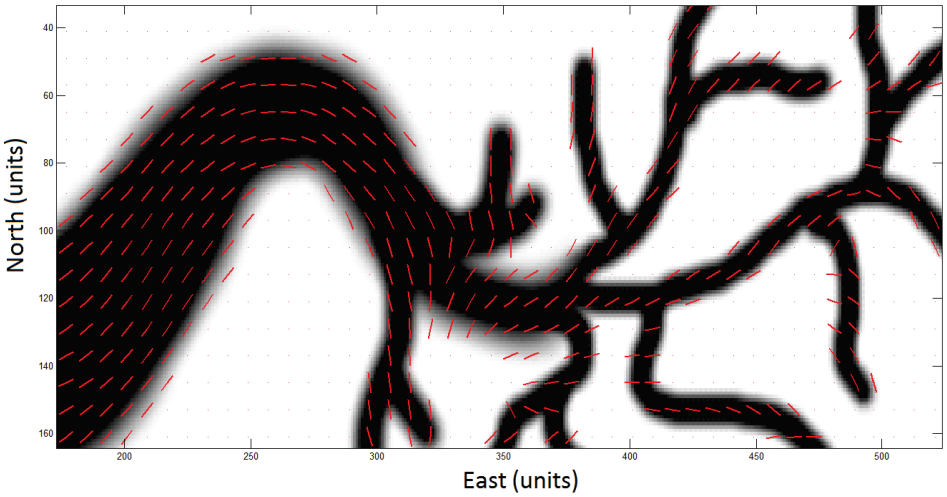

(b)

Figure 3.6: LVA field generated using small and large window (a) and (b).

A 3D implementation of the adaptive technique is shown in Figure 3.8. A cross section about

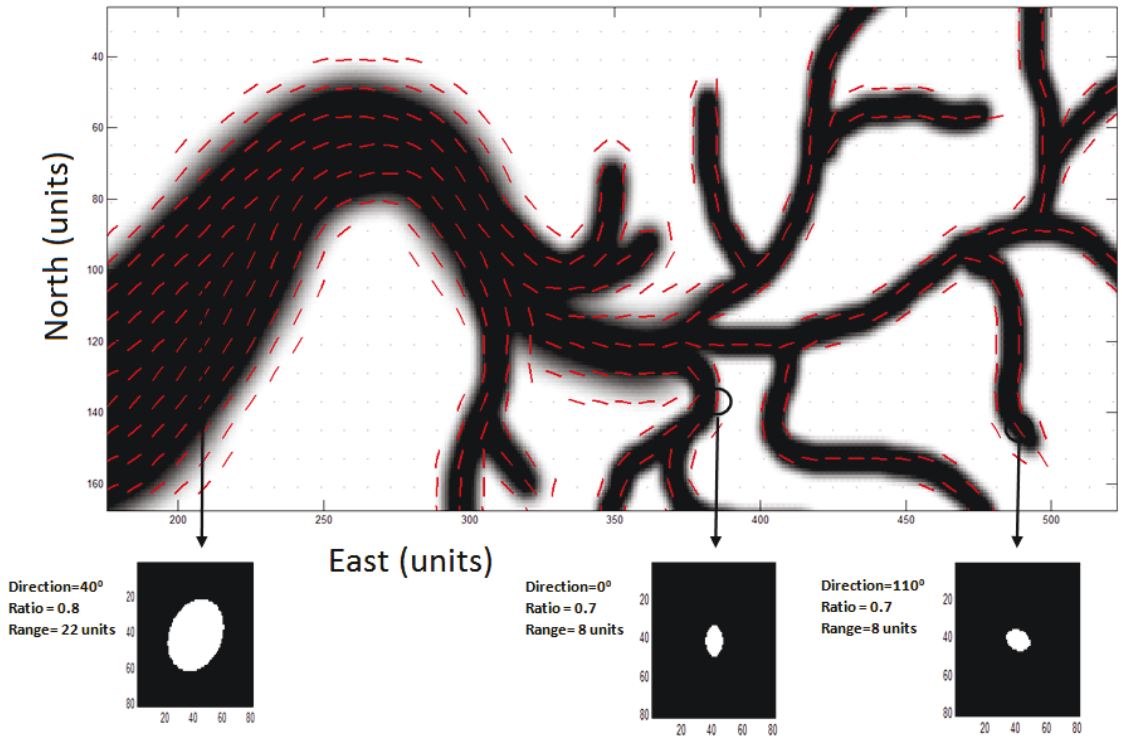

Figure 3.7: LVA field generated using adaptive windows and the sizes of the ellipsoidal search area at three points are highlighted. The major axis of the ellipsoid is allowed to vary from 8-80 units, ratio of semi minor to semi major had a range of 0.2-1 and the angle of rotation (θ) varied from $0 - 180^{\circ}$.

z-axis shows the LVA at different scales.

The term reliability (R) is used here as an index of confidence or accuracy (Juelin and Moreaud, 2008) on the orientation derived from a structure tensor. An estimate of reliability $R = 1$ underscores the presence of a strong local anisotropy. The reason is that when gradient vectors are unified along a clear dominant direction, the eigenvalue associated to the least gradient change, i.e. λ_2 approaches zero and $R \rightarrow 1$ (Feng , 2003). When $\lambda_1 \approx \lambda_2 \gg 0$ there is no preferred direction of local intensity change that suggests an isotropic region.

For the purpose of this work it is considered as a measure of anisotropy magnitude in a local search window. So a degree of certainty can be associated when computing an angle of local orientation. In that regard it maybe sufficient to characterize local anisotropy within a stationary zone through the adaptive window treatment by selecting the window size corresponding to the largest R. Isotropic features within the domain can be identified through orientation tensors - where the intensity variation has no distinct direction nor a significant variation of components. As mentioned before, the local structures are closely related to the local orientation in order to pick the most relevant feature of a neighbourhood. In these cases setting a threshold of $R \leq C$ helps to identify isotropic zones and the local anisotropy ratio is set to 1:1. The choice of the constant C can be assessed by choosing a reasonable cutoff value of the reliability measure. For instance in the evaluation of LVA fields for an exhaustive seismic survey local structures maybe diluted by the presence of noise and it is reasonable to mark areas as isotropic when there is low confidence in the ascertaining the degree of anisotropy.

Depositions in nature are characterized by complex geology and usually do not reflect the assumption of constant anisotropy magnitude throughout. Typically prior to property modeling exhaustive rock models are generated in order to demarcate stationary zones within which the statistical properties (i.e. constant mean, variance) of the data are assumed to come from the same distribution. Once the stationary zones have been established the nature of the boundary itself must be accounted for (Larrondo and Deutsch, 2004). The boundary can be referred to as hard or soft. Hard boundaries are found where there are abrupt changes to the spatial statics such as the mean or variance reflected in the alteration of mineralogy or grade. Soft boundaries on the other hand contain a transition zone where the statistics vary smoothly. In dealing with geology separated by hard boundaries the standard practice is to subdivide the modeling area into stationary zones and apply a moving window or the adaptive window framework to assess the LVA field. This allows the users to customize the parameters of the search neighbourhoods (i.e. the six parameters needed to define and ellipsoid window in 3D) for the generation of LVA field at each of the stationary domains.

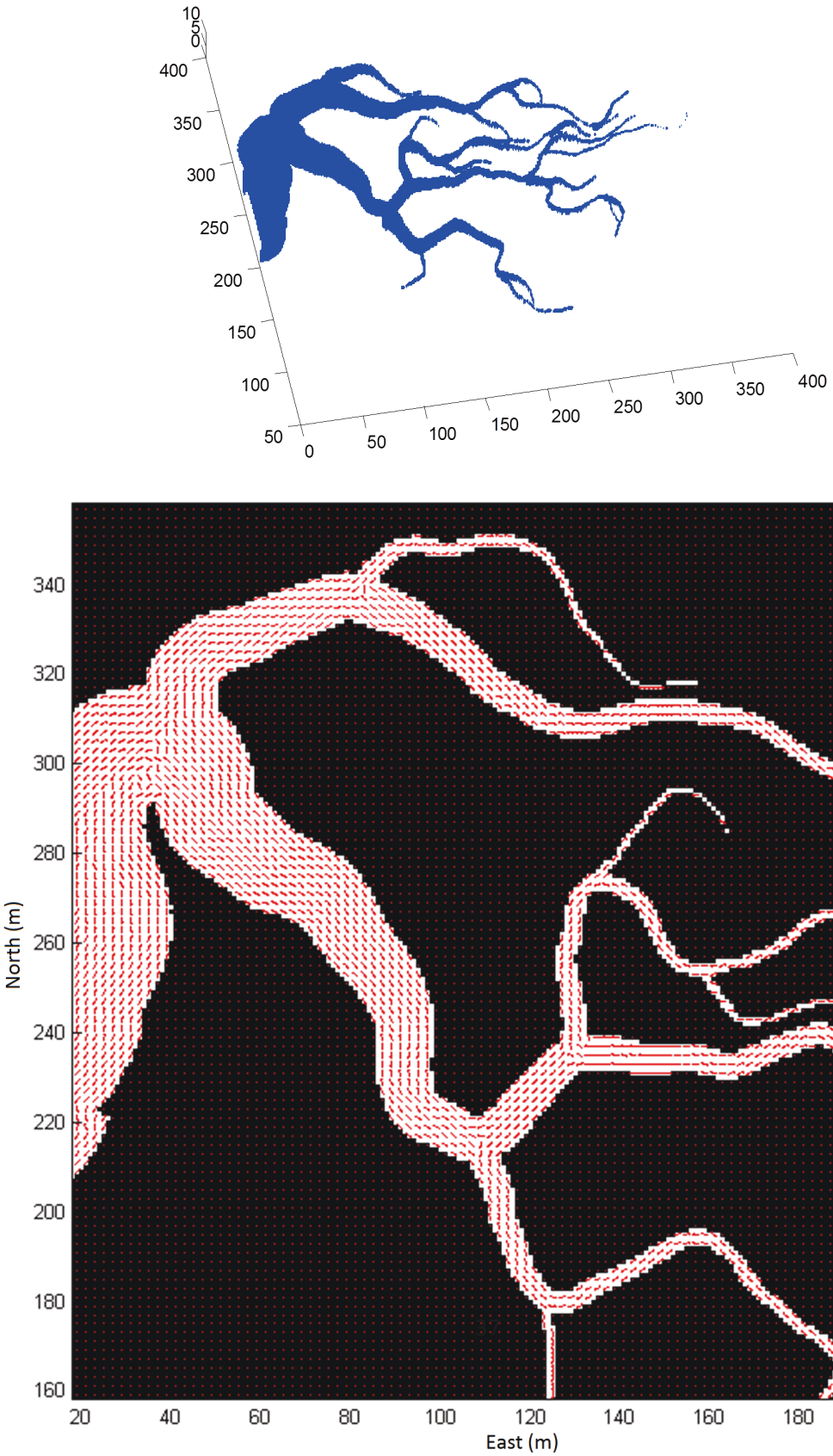

Figure 3.8: Cross section through the Z-axis at z=9 of the 3D fluvial model (top).

The nature of the transition between two stationary domains has significant modeling implications (Wilde and Deutsch, 2012). The soft transition boundary would show pronounced nonstationary behaviour of the spatial statistics associated to property of interest. Such characteristics are found near increased fractures between the boundary of the partitioning structural domains such as faults or brittle zones (Larrondo and Deutsch, 2004); and also common in porphyry style copper mineralization where the change in the local mean across the boundary is continuous (Ortiz and Emery, 2006). In this case the transition zones needs to be identified and in building a LVA field the geological property across the domains has be to maintained. The assumption of a constant anisotropy ratio no longer holds in the nonstationary transition zone as they are strongly influenced by their location relative to the boundary and so the anisotropy ratio must be allowed to vary smoothly across the regions.

3.3 Generating LVA from Geological Bodies

Large scale issues with stationarity are often accounted for by generating a geological (categorical) model that delineates major domains within the deposit. Modeling complex deposits, like fluvial channels in reservoirs or vein type deposits for example, are particularly important as these types of features distinguish domains with very different statistical properties. The geological model often contains significant information on the local orientations of properties within the domain. Once these geological models are generated, they can be processed to extract relevant LVA information so that property modeling within the geological domains is consistent with the shape of the domain. Here, morphological thinning techniques are used to generate 'skeletons' of the original geological model which are used to indicate local orientations at a larger scale. The previous approach with local windows could also be used but thinning is more appropriate for very large scale features that would require unusually large window sizes.

Thinning algorithms are well known image processing techniques that have numerous applications in pattern recognition, data compression and data storage (Gonzalez and Woods, 2007). It is a morphological process that codes specified object pixels to the background in binary images and gives a compact shape representation (skeleton). Once the boundary points have been identified, an object is eroded layer by layer until only a skeleton is left. The skeleton is defined by the medial axes of an object. In Euclidean space the median axis is a set or loci of centers of maximal inscribed spheres (circles in 2D). Maximal spheres (or circles) are such that they are contained within the object but not entirely covered by another sphere. The exact computation of a medial axes is non-trivial (Wang and Basu, 2007). The methodologies presented here are template based

iterative thinning techniques that give the approximate medial axis.

3.3.1 Centerline Extraction with Iterative Thinning

The first criteria of thinning is assigning a value of 1 to all object pixels and a value of 0 to the rest of the coordinates in the domain. The pixels containing zeros form the background are in a stable condition, i.e. a point with zero value is never transformed to 1. The object undergoes the thinning operations as it iteratively removes some object coordinates until the specified condition of a skeleton is reached. Most thinning algorithms in literature are parallel (a set of object voxels are coded to zero at the same time), but differ in the manner of organizing an iteration step. The 2D thinning algorithm, K3M is developed by Saeed et. al. (2010) is a sequential iterative method that will produce a thinned one pixel width skeleton.

Geometry conservation is an important aim in all thinning algorithms. Accordingly, the K3M (Saeed et al, 2010) removes the image pixels while the image structure is preserved. It consists of a series of six phases which subsequently decides which pixels to keep and which to remove. In the first phase the border pixels are marked (pixels that stick out into the background), and this is the basis for the thinning phases. A 3×3 neighbourhood around a border pixel is selected and thinning decisions are made only at these pixels. The front moves inward iteratively.

The advantages of the algorithm are that it preserves the right angles at the lines interconnections, which ultimately result in better correspondence between the original and the modified image. The iterative thinning is shown in a synthetic 2D example in Figure 3.9.

The methodology proposed by Palagyi and Kuba (1999) is used in 3D. The order of removing the border points prescribed by Palagyi and Kuba (1999) is symmetric and therefore the skeleton is geometrically at the 'middle' of the original object. The implementation by Min (2011) is used. It is recommended that before applying thinning techniques the data is smoothed and MAPS technique (Deutsch, 1998) is used in this case to generate a more consistent and smooth centerline. In generating the LVA, the centerlines/skeletons are fit with splines and the local orientations are found from the spline gradients (Figure 3.10).

The process of spline fitting to thinned centerline involves a few steps but easy to implement. Consider the thinned structure in Figure 3.10c which is generated from a compact 3D model. It is clear that this rather complex and largely connected structure needs to be partitioned before interpolating the geometry with splines which can be done in an iterative manner (Figure 3.11). A single branch of the skeleton is tracked, i.e. coordinates of a branch are gathered and stored in an array, from one end point to another. Since the skeleton is always one-pixel wide, all end points

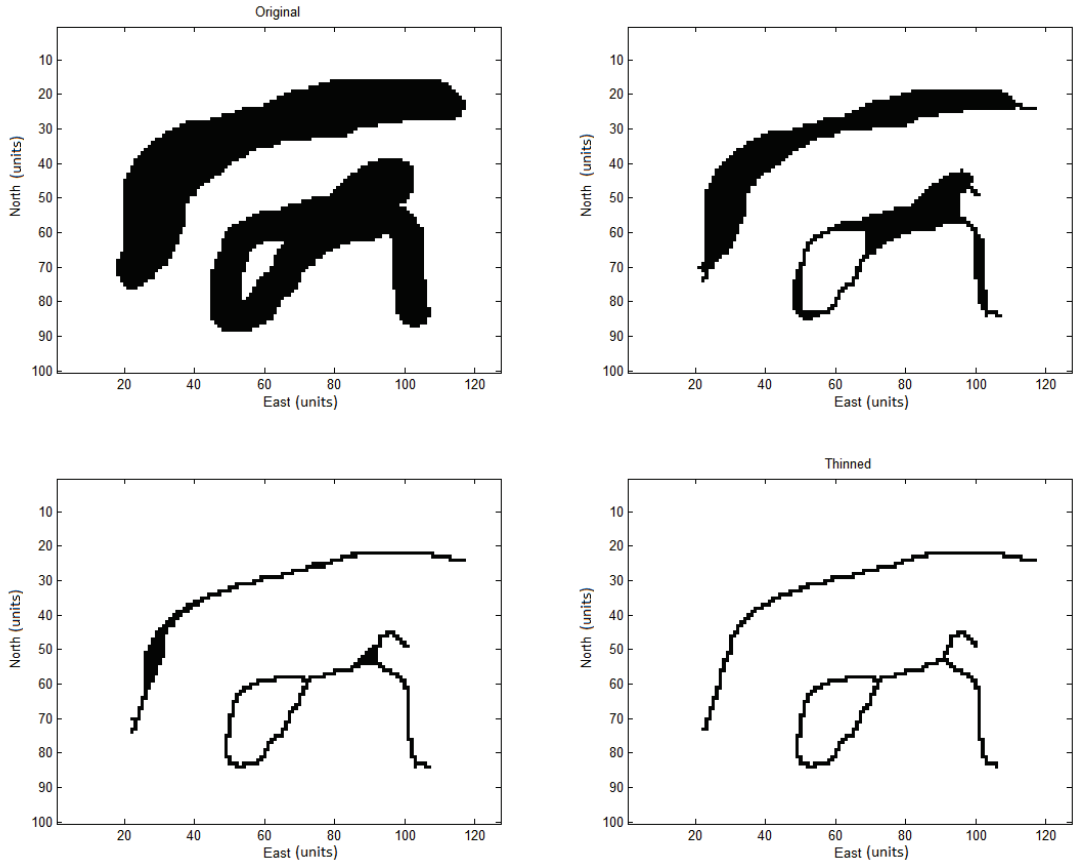

Figure 3.9: Iterative thinning by K3M; different stages into skeletonization shown.

are marked by a single object pixel about a 3×3 neighbourhood ($3\times3\times3$ cubic area in 3D). A spline is now fit to the array of coordinates and the process continues until all skeletal coordinates have been replaced. In subsequent steps a new end-point is identified after the section of the skeleton that is tracked is removed from the initial skeletal array. Thinned skeletons of a simpler object in Figure 3.9 are detached and so the end-points easily identifiable. Here, several instances of piecewise splines fitting to the original skeleton are shown (Figure 3.11). In a branched out and largely connected skeletons this iterative approach can be applied which results in a smooth interpolation of compact body's underlying structures and subsequently an exhaustive LVA field can be determined (Figure 3.10d).

In literature, connectivity preservation apart from maintaining the topology in a huge concern for thinning algorithms and almost all seek to achieve this. But for the purposes of evaluating LVA

of a geologic body this may not be significant criteria. The thinning algorithms alone do not generate a smooth LVA field through centerline extraction. There may be instances of unwarranted protrusions and bifurcations in thinned skeletons not consistent with the apparent connectivity in the original object. This can be overcome by image smoothing by MAPS. Consequently this also raises the concern if the original object is too smooth that is deviates from the original geometry, that is why trial and error through the parameters of MAPS is done to obtain a reasonable smoothing. It is shown that that preprocessing can greatly improve the resulting skeleton. Another way to deal with undesirable features in the centerline is to clean the centerline i.e. rectify unnecessary branching of the thinned skeleton. The cleaning step is implemented along with the k3m technique to remove any irregularities caused by iterative thinning and is discussed in Chapter 5.

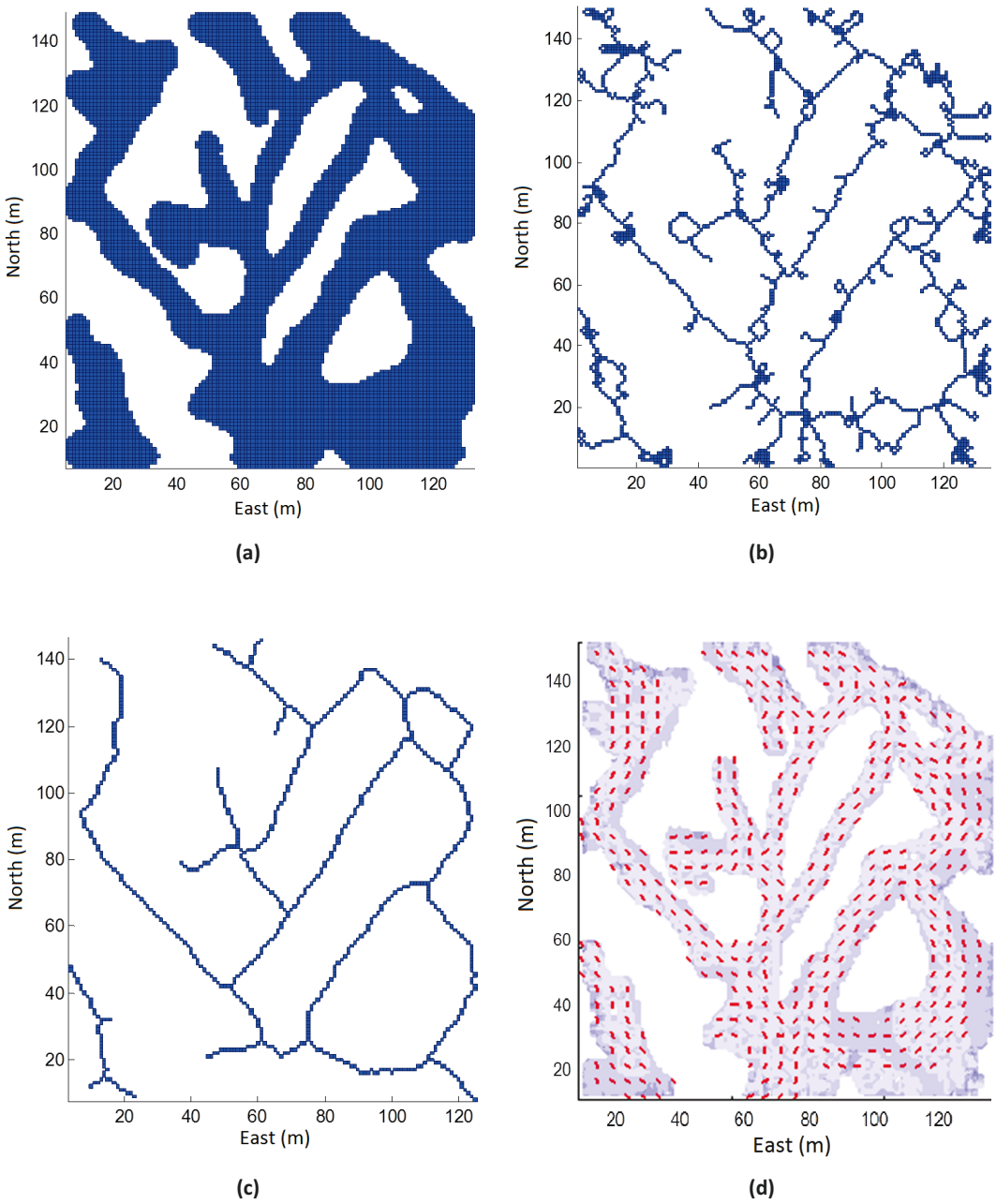

Figure 3.10: Thinning in 3D using the 8-subiteration technique: (a) shows the model after smoothing by MAPS, and (b) is the resulting centerline obtained without smoothing the binary model; (c) centerline generated after processing data with MAPS; (d) LVA field for the 3D geologic body from the centerlines. The centerline (b) is fitted with splines to obtain a regular and smooth trajectory. LVA field orientations are taken tangential to the spline and the model is populated by standard moving window technique.

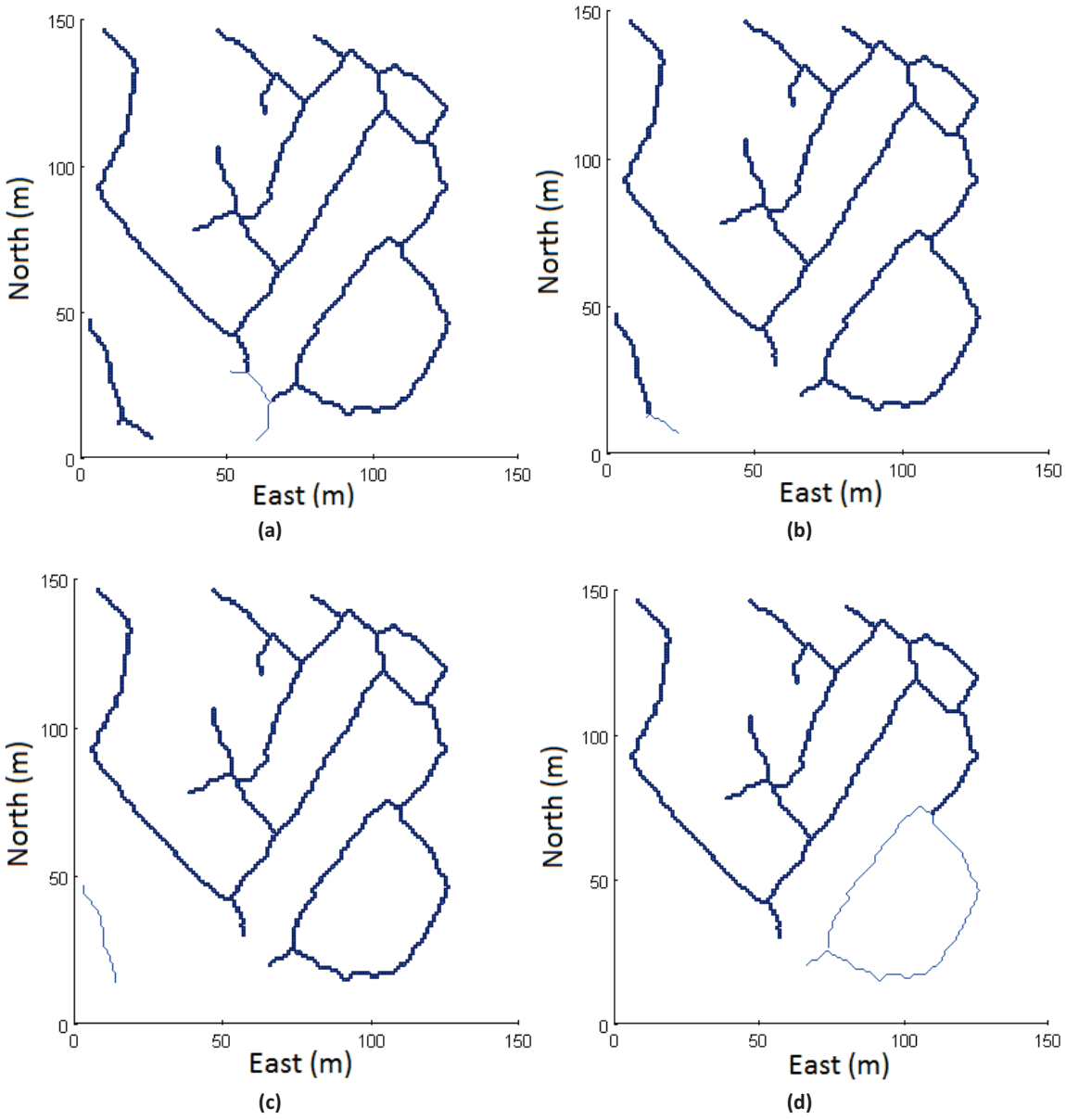

Figure 3.11: Iterative tracking of each section of the original skeleton before fitting the identified branches with splines. A section of the skeleton goes from one end pixel to another, and using one-pixel wide skeleton ensures each pixel only contributes to the trajectory of the initial object geometry.

Chapter 4

Combining LVA Fields

Generation of an LVA field is often data specific and it may be necessary to consider multiple data sources to generate a single field map. Distinct LVA maps can be generated from different sources (a practitioner's manual interpolation, remote sensing etc) become available. The next concern is how to combine the different anisotropy fields into one meaningful map. Such merging of information - a form of averaging - is used in fields of computer vision to obtain a final representation which can be assigned a higher degree of certainty than any individual statement (Granlund and Knutsson, 1995). The measure of certainty in LVA fields can be interpreted from the parameters that define the anisotropy magnitudes. Ideally local orientations should be consistent with the major direction of continuity. In order to define how well the local structure is captured a scalar descriptor associated with the orientation vector can be used. The reliability (R) measure taken here is a scalar quantity and defines the confidence level in the available information.

Consider the example shown in Figure 4.1, where the gradient-based technique is used to estimate the local feature orientation. Where the image signals are clear the index of confidence $R = 0.997$ (reliability) is high; with the presence of Gaussian white noise the signal interpretations becomes more ambiguous and the measure of confidence decreases and as noise increases,. As a result the features lose most of their integrity, the confidence in the orientation is poor. Similarly a factor of reliability on the LVA orientation can be interpreted as the measure of anisotropy.

Several techniques such as the gradient or PCA based extraction of local orientation generate LVA fields as discussed in Chapter 3. The information on local structure is represented through tensors. Eigen-decomposition of the tensor gives the orientation at an estimating point. These structure tensors can also be exploited to combine local orientations. To illustrate the notion that LVA averaging cannot be treated as simple vector averaging the following cases are shown (Figure 4.2). Instead of vectors, LVA information is merged through its higher order counterpart i.e. by

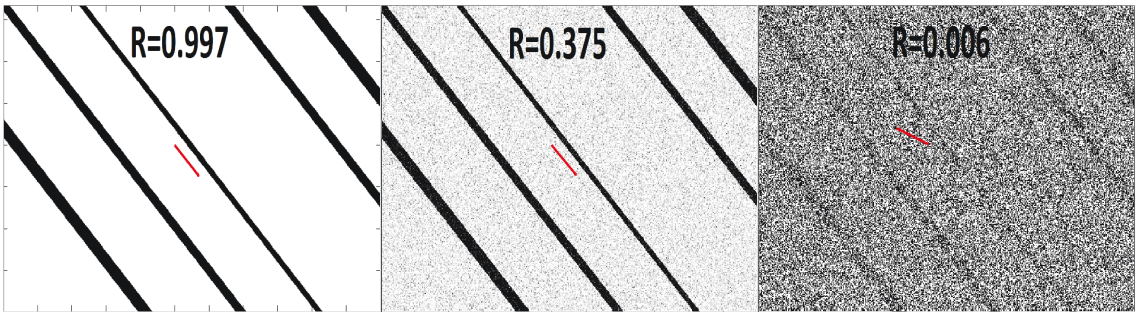

Figure 4.1: Local orientations calculated with the gradient-based technique and associated measures of confidence the directions shown. The corresponding R values suggest how dominant the principal orientation is compared to its orthogonal component. Dimensions are 500×300 units. Reprinted from Figure 3.5.

tensor averaging. Some basic and necessary properties of merging various LVA fields need to be established before looking at combining orientations.

1. Combination of similar orientations, i.e. along the same axis, should lie on the same axis of orientation ; the polar nature of LVA fields is important

2. Zero information combined with itself is zero or no information

3. Contradictory information on orientation should result in no information

From Figure 4.2 it becomes apparent that vector combinations do not have the desired properties expected in an LVA combination scheme. Vector combination does not honour the axial nature of the LVA orientations, thus tensor based averaging is considered (Figure 4.3). In terms of vector combinations the normalized weighted averaging is:

$$v_m = \frac{\sum R_i v_i}{\sum R_i} \tag{4.1}$$

The term v_i are the different cases of vectors being considered, and R_i are index of confidence associated with each vector.

Since the norm of the mean vector v_m varies between 0 and 1 the procedure is known as the normalized averaging (Granlund and Knutsson, 1995). For the relevant case averaging is done with tensors (T) the formula is:

$$U_N = \frac{\sum RT}{\sum R} \tag{4.2}$$

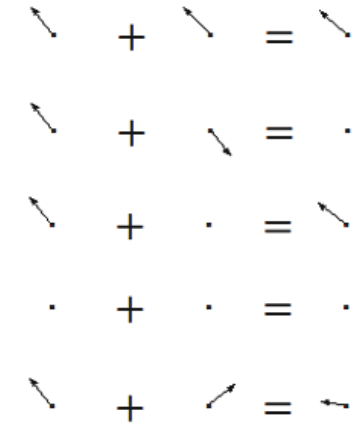

Figure 4.2: Vector averaging of orientations show that the axial nature is not honoured (second row from top); moreover conflicting information does not result in no information.

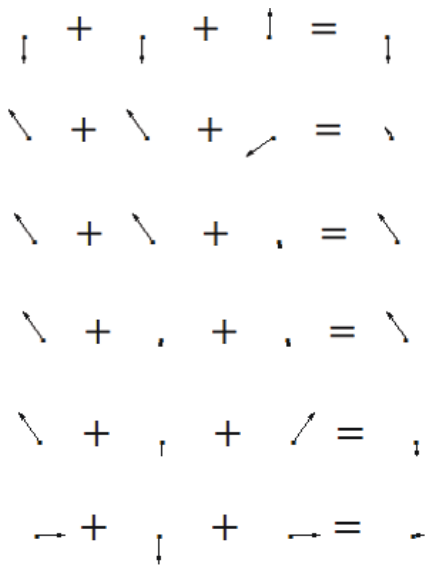

Figure 4.3: Tensor based combination of local orientations follow the necessary rules as laid out here.

where T represents the relevant tensors, and U_N is the normalized average tensor.

Tensor based combination is illustrated on an example having three distinct LVA fields. The underlying map represents the mean rainfall in the state of Hawaii for the month of January 2011, where the colour gradations are discretized rainfall categories shown in Figure 4.4 (Giambelluca et al, 2013). The first case of LVA field is obtained using gradient based moving window technique discussed in Chapter 3. The two other LVA fields are generated from different manual interpretations. For these cases smooth splines are fitted at manually selected discrete locations and next moving window techniques are applied whereby the LVA orientations are taken tangential to the spline. A more elaborate discussion on LVA field inference in this manner is given in Chapter 5. Distinct estimates of the LVA fields provide contradictory information on the direction of anisotropy at several regions which requires a user's judgement before consolidating the local orientations from different LVA fields. The user must assign the value of weights for each of the input LVA fields needed for tensor based orientation averaging.

From Figure 4.5 it is evident that if the input LVA field orientations are smooth and follow the underlying gradation of properties, the tensor combination of the LVA fields is reasonable. Also, this is a reflection of the measure of confidence given to each inputs LVA fields in normalized tensor averaging . However, there are regions where local orientation is not consistent or there are features with discontinuities and orientations do not vary smoothly from one pixel to the next as shown in the highlighted area in Figure 4.5 (bottom, right).

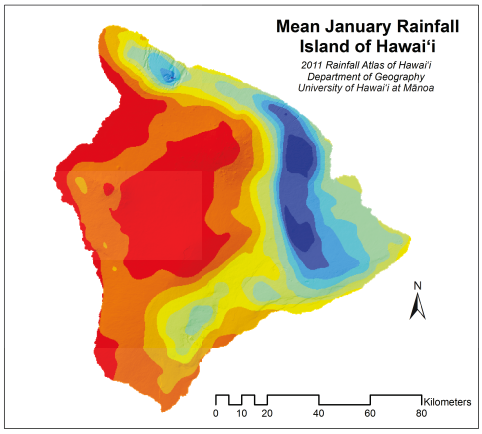

Figure 4.4: Colourmap of mean rainfall for the State of Hawaii taken over a single month (Giambelluca et al, 2013).

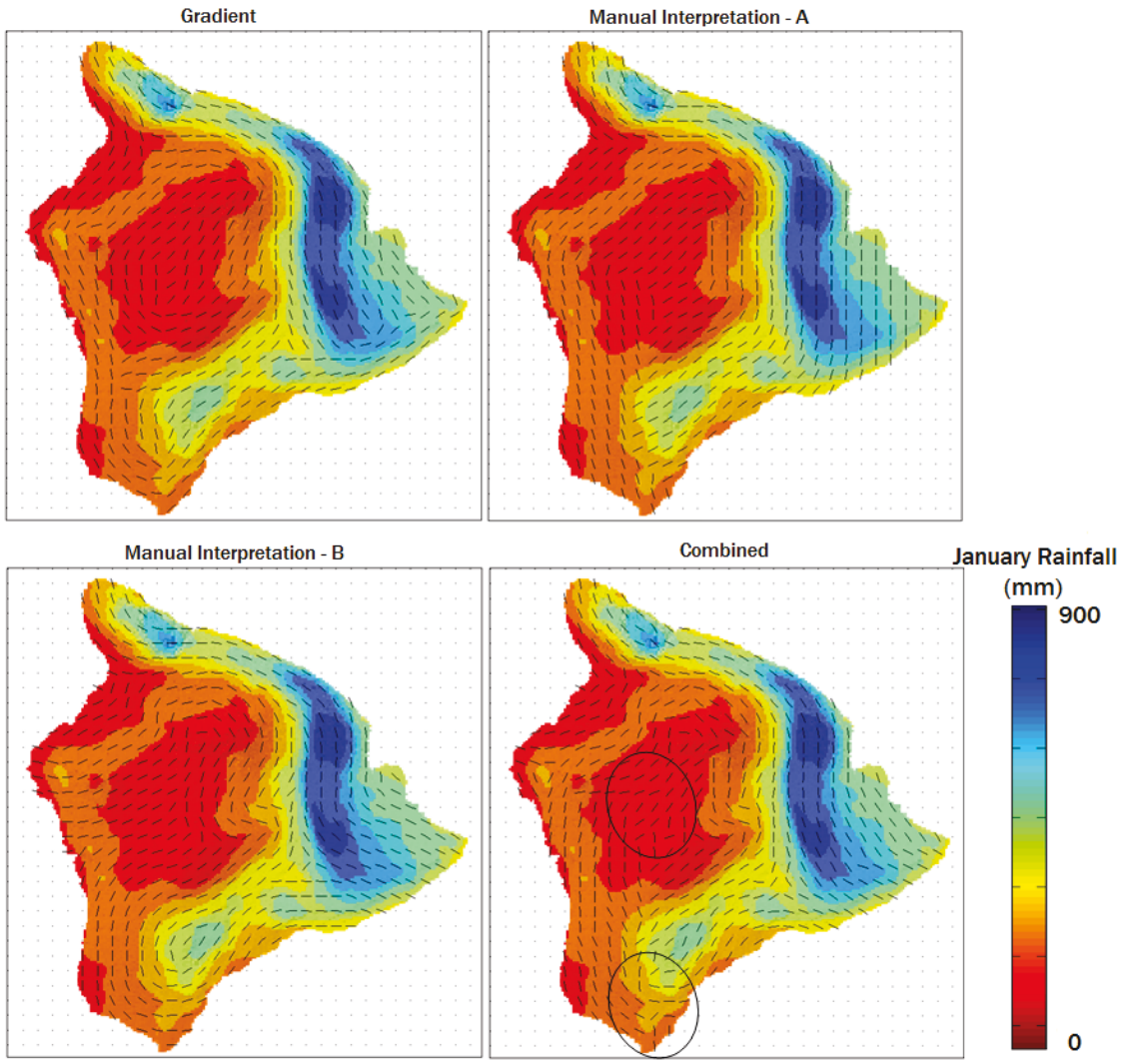

Figure 4.5: Three distinct LVA interpretations are presented. By giving weights to input LVA the user determines what characteristics of the input are retained in the combined LVA field. Inconsistencies present in initial LVA representations can be carried though to the final inference. Plot dimensions are 200×225 km. The higlighted are areas of high local angle irregularity.

In this example result suggests that there is still room for improving the combined LVA field, as the LVA orientations are irregular is some areas. This could happen for several reasons: (1) the input LVA fields themselves did not contain orientations that were locally smooth and consistent in their small neighbourhood; (2) one or more LVA fields had distinct representations owing to feature discontinuities. It becomes clear from this small example that automatic tensor combinations may

not always be a reliable form of LVA combination. There is a need to develop a methodology that will reduce these problems. As a starting point the three initial LVA field derived from different methodologies are considered. A fourth LVA field of the combined tensors is also considered as the base case which will be improved. Updating the combined LVA field to be locally smooth is done by:

Step 1. Identify the inconsistent regions in the combined LVA map

A. Locate points where the orientation at the node is markedly different than its neighbours using circular statistics or using sum of pairwise dot products. This is achieved by calculating the angle variance and nodes with high angle variance attribute to problematic regions (Figure 4.6)

B. Inconsistency in local orientations can also be determined from the measures of dot products and is easy to compute (Figure 4.7). If the axial configuration of the surrounding orientations are similar, the value of S by equation 4.3 is close to 1, and the local orientations have higher stability

Step 2. Visit every location in the combined LVA field randomly and only once, decide either to keep the existing angle or substitute with orientations from the initial LVA maps

In Figure 4.5 (bottom,right) the local inconsistencies present in the combined map indicates that weighted tensor averaging does not yield the smoothest LVA interpretation. It could be influenced by strong regional discrepancies in angle direction in the initial LVA fields and so searching for better estimates within input LVA maps is also not ideal.

C. Instead a better procedure is to generate a set of orientations from the given LVA fields - i.e. build a larger list of orientations to choose from in the substitution process (Table 4.1)

D. Consider the synthetic example shown before. The larger list of orientations can be created considering the 2-orientation averages between the initial three LVA fields and one 3-averaged angle. Now, for every pixel there is a library of 8 different orientations to choose from

Step 3. Substitute the most suitable orientation from the library based on the minimum angle variance or maximum angle stability (Figure 4.8)

Step 4. Once all the nodes are updated, visit the points randomly again until no more improvements on the value of reliability (R) can be made.

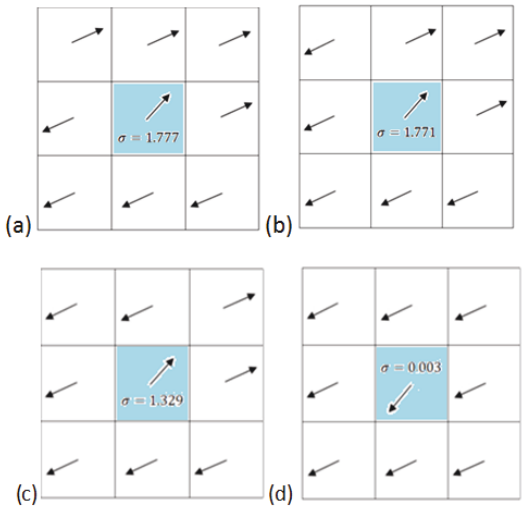

Figure 4.6: Identifying inconsistent regions by finding the angle variance locally. The axial nature of the LVA orientations must be accounted for prior to calculating the angle variance. This involves 'flipping' the orientations (considering the opposite orientation axis). Smallest angle variance is obtained when the same polar configuration is reached.

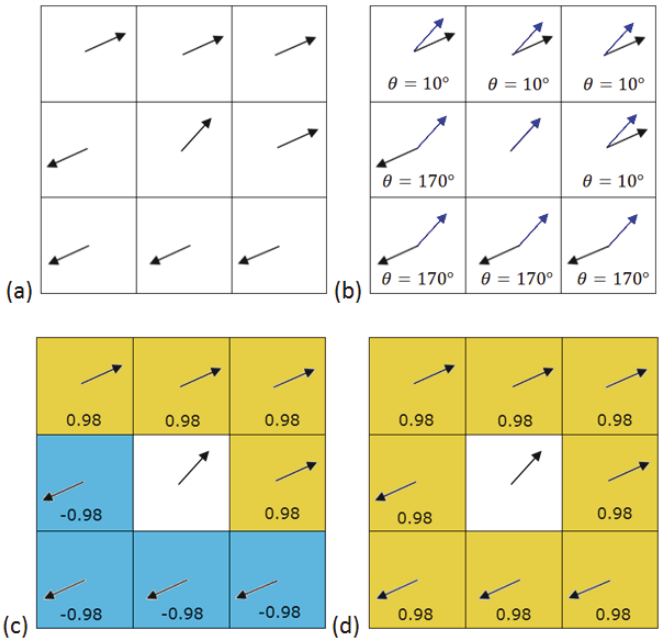

Figure 4.7: Identifying whether the orientation in the central node is different to its nearest neighbours by dot products. Pairwise dot products of similar orientations have values close to 1, and -1 if they lie on the opposite axis of orientation. The value of angle stability S (normalized pairwise dot product) is approximately 1 indicating the central orientation is consistent in its region.

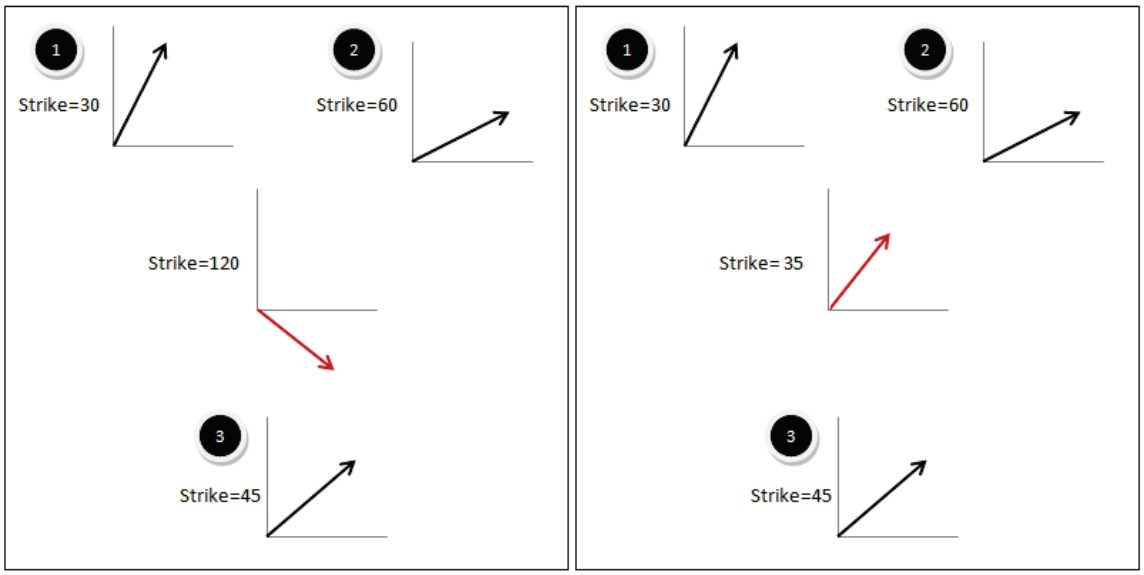

(a) **(b)**

Figure 4.8: Orientation shown in red at the central node is locally inconsistent as it is characterised by a low angle stability value (S = 0.25). By checking all the orientations in the library (Table 4.1) the angle configuration of high local consistency is achieved. The initial orientation (strike 120) is substituted by strike 35 from a list determined for the current location.

Table 4.1: A library of orientations and list of associated local angle stability for the example above. The orientation with the highest angle stability is selected.

Angle List	Local angle stability (S)
10	0.80
35	0.96
70	0.89
150	0.75

Implementation Issues

In using the angle variance as a measure to select suitable orientations, some additional steps are required. The angle variance of the cloud of orientations does not consider the axial nature. For any given set of orientations where some of them are directed in the positive axis (α) and other in

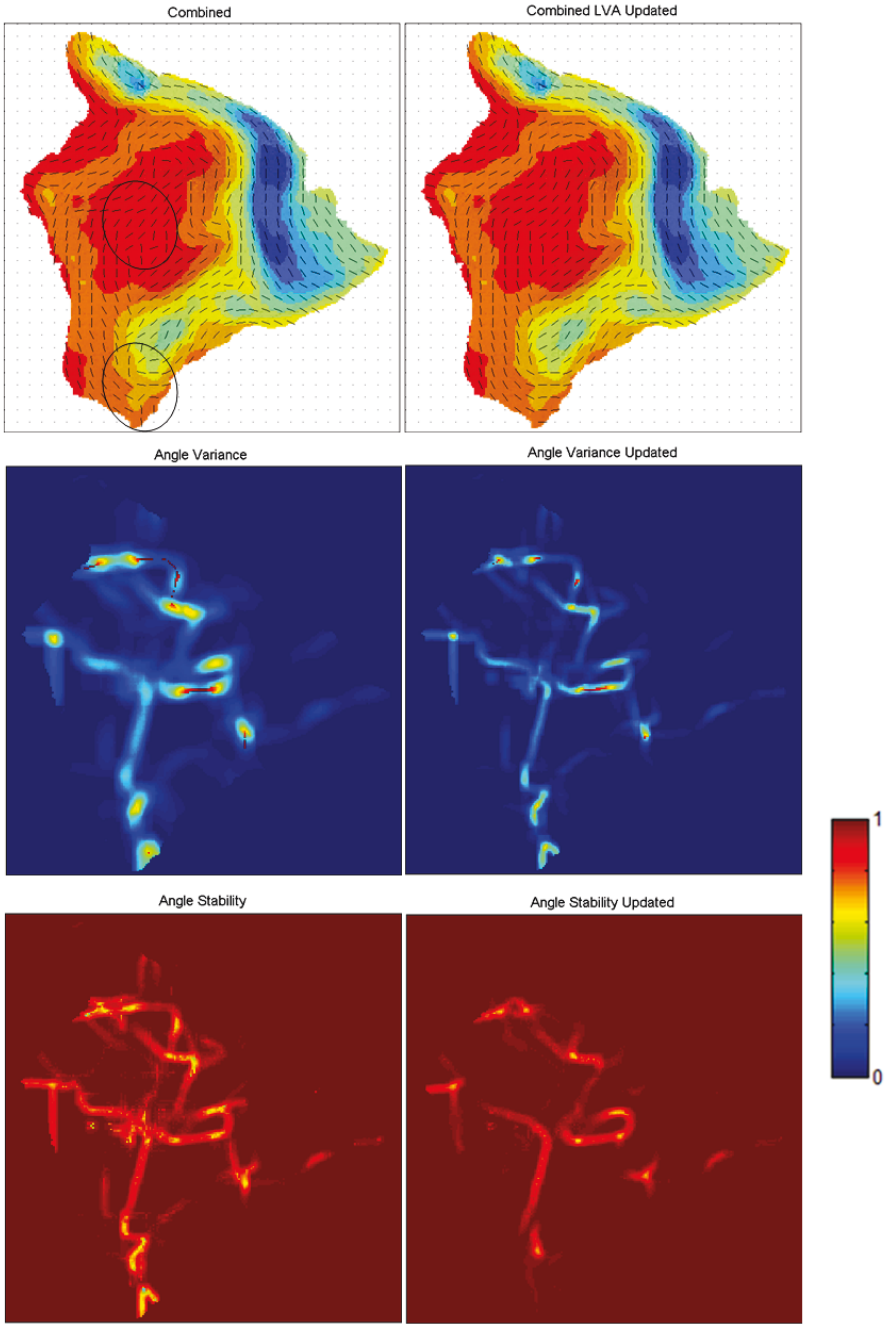

Figure 4.9: The top left LVA field is the initial combined case (Figure 4.5) and is taken as the case to be improved on. Note the highlighted LVA orientations after updating is more consistent. Building a larger list of orientations yields a smoother interpolation of LVA field. The two plots of angle stability and angle variance show that the inconsistent regions is reduced in the final LVA map indicated by higher angle stability and lower angle variance in the updated maps. All plot dimensions are 200×225 km.

the opposite axis ($\alpha + 180^{\circ}$) the resulting angle variance would be uncharacteristically high (Figure 4.6). In order to tackle this problem the 'flipped' orientation is considered. By flipping the local orientation can assume a state of axial configuration that gives the minimum circular variance. The minimum of which is obtained when most or all the orientating are along the same pole.

From Figure 4.6(a) it is easy to see that although the central orientation points to the opposite axis, it nonetheless represents a state where the central orientation is consistent locally. However this can be only confirmed until stage Figure 4.6(d) is reached. This iteration of flipping each orientation in the neighbourhood can be avoided by considering the angle stability criteria.

In the dot product case consider the same setup as in Figure 4.6 (a), the calculation involves estimation of the pair wise dot product of the central orientation to its neighbours. The LVA map contains orientations that are of unit length, this means that each of the dot products will vary from -1 to 1. Next only the modulus of the pair wise dot products is considered. By using the dot products the index of stability or consistency of the central orientation with respect to its neighbours can be defined as :

$$S = \frac{\sum \text{modulus of pairwise dot products}}{\text{number of pairs}} \tag{4.3}$$

where, S is bounded by 0 and 1

Consider the scenario where there is a well defined LVA field and it needs to be incorporated into the combinations described so far. Then the LVA field orientations can be easily coded into a tensor. Geometrically we see that a tensor is described by the eigenvalues. So, given the orientations and ranges of anisotropy exhaustively a tensor from this information can be easily constructed:

$$P = \begin{bmatrix} cos(45^{\circ}) & cos(45^{\circ} + 90^{\circ}) \\ sin(45^{\circ}) & sin(45^{\circ} + 90^{\circ}) \end{bmatrix}$$

$$D = \begin{bmatrix} 10 & 0 \\ 0 & 1 \end{bmatrix} \tag{4.4}$$

$$T = PDP^{-1} = \begin{bmatrix} 5.5 & 4.5 \\ 4.5 & 5.5 \end{bmatrix}$$

This section summarizes the methodologies that have been developed to identify how to best generate a single LVA field from several inputs. This is an exercise in averaging where the goal is to generate a smooth LVA field that explores the methodology of deriving the most information

from input LVA fields which is prudent in situations where there is little confidence in one or more of the inputs. Tensor averaging along with the generation of an exhaustive local list of orientation is a practical method to bring smoothness (in an LVA field) without the deficiencies that may be present in the initial LVA fields. Two ways to measure local angle inconsistency are presented. Similar regional inconsistencies are identified by both the methods in the combined LVA field (see maps of angle variance and angle stability in Figure 4.9), and this allows the user to verify the results when using either method. However, angle stability is more straightforward to implement as it is able to rectify an inconsistent location by quickly identifying the correct axial nature in the search area.

Chapter 5

Case Study

The purpose of this study is to evaluate techniques for the generation of LVA fields. Accurate predictions of nonlinear complex depositions are difficult to achieve using traditional methods such as kriging. The limitation arises when geological heterogeneity is curvilinear and cannot be captured well through standard variogram modeling where only a single direction of continuity is assumed. By considering LVA fields information from nonlinear anisotropy can be incorporated to bring more realism into modeling.

One way to incorporate non stationarity into estimation techniques is to first build an LVA field of the modeling domain. Boisvert and Deutsch (2011) propose a methodology that uses nonlinear paths to incorporate LVA with kriging, and it is necessary to generate a well defined LVA field prior to estimation. In the context where direct measurements are sparse and spatial features are not apparent from the data, kriging with LVA can be used for modeling. The LVA field itself can be generated from analogs or exhaustively sampled secondary data etc. This section presents several techniques for the inference of LVA fields in a copper porphyry deposit and applies kriging with LVA (Boisvert, 2010) to build a 3D model.

5.1 LVA for Copper Porphyry Data

Blasthole data from a copper porphyry deposit is considered in this analysis. Original samples have been normalized to protect its identity; spatial distributions of data are unaltered. Several approaches are explored for generating an exhaustive LVA field before considering geostatistical modeling. The data (Figure 5.1) shows clear nonlinear features where it is difficult to assume a single direction of anisotropy. Instead second order non-stationarity is introduced though the generation of a LVA field. This study looks at four methods of generating the LVA field by, (1) the

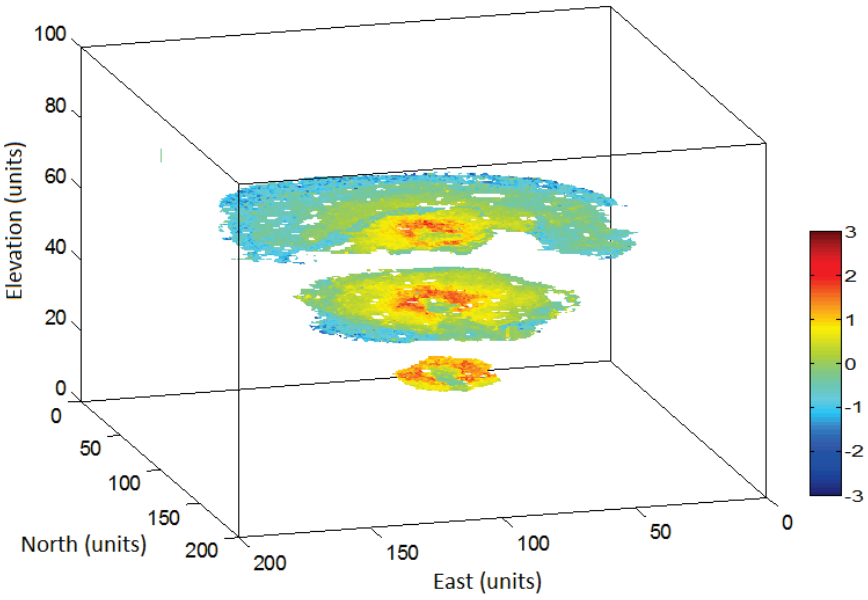

Figure 5.1: Copper porphyry data shown at elevations 20 m , 40 m and 60 m. The high grade mineralization zone at the center (red-orange) shows ellipsoidal dispersion, surrounded by low grade zone (blue-green).

extraction of 2D centerlines from distinct layers using thinning algorithms, (2) manual polyline fitting, (3) fitting radial shape parameters and interpolating for the 3D model, and (4) extracting local orientation by a moving window technique presented in Chapter 3.

GSlib style grid format is used and a cell size of 15 m considered in x, y and z directions. The modeling area is $153 \times 180 \times 84$ of 2,313,360 cells.

5.2 LVA Field from 2D Thinning

The data is sparse so a smooth map is first generated with block kriging. Where the data density is sufficient and depicts the geology well, anisotropy of high grade mineralization shows a prominent horseshoe like pattern (elevation 40 m) morphing into radial structure at higher elevation (60 m) as seen in Figure 5.1. Densely sampled blasthole data is available from the copper porphyry deposit at elevations greater than 30 m. At lower elevations (below 10 m) data is sparse and no distinct structure can be observed. The end objective is to predict the ore values to the bottom of the final pit where the LVA is inferred from existing data.

2D sections of the deposit are considered for LVA field generation. The goal is to construct

polylines that mimic the general shape of the deposit using the densely sampled layers, then interpolate the geology where data density is sparse. Once a smoothed map of the data is obtained the estimated 2D sections can be split into two distinct zones, (1) an ellipsoidal high grade zone at the center and the (2) surrounding low grade area (Figure 5.2). Across several meters in the vertical the style of mineralization varies gradually and the treatment of feature extraction is applied at mining benches 10 m apart.

Thinning involves peeling layers off an object until the thinned representation is found and details of the thinning algorithm applied here is discussed in Chapter 3. In order to capture the distinct zones of grade distributions the 2D section is binary transformed by considering several cutoff values. The cutoff values for the zones are specific to each elevation and are found by trial and error before selecting one that resembles the desired structure. For this process a practitioner needs to examine plan sections at several elevations and assign cutoff values so that the true mineralization style can be captured. Binary conversion assigns data values in the cutoff region are as 1 and outside as 0. The selection of the cutoff values is critical as the transformed model should be a good approximation of the underlying geometry (Figure 5.2). Thinning techniques are applied to this binary data that involves iteratively removing the outer pixels of the object at controlled stages until the thinned representation is left. The sequential iterative K3M algorithm (Sayeed et al, 2010) is used here as it provides a stable centerline representation especially considering the radial nature of the mineralization zone.

Basic workflow

1. Block krige the normalized (Cu) grade data, to arrive at a smooth map so that the spatial characteristics of the copper grade are discernible. A block size of 15×15 is used here and the anisotropy ratio considered throughout is 10:1

2. Select cut-off values that give the 'best' visual shape representation of the original structure. Ensure that the important characteristics are within the cut-off range and binary transform the model

3. Thinning algorithms may generate artifacts in the centerline if the binary data has irregularities such as missing data, or the data are too disconnected. Binary transformed data is processed through image smoothing filters to reduce irregularities. Centerlines are extracted using k3m.exe, and the Gslib program maps.exe (Deutsch, 1998) provides smoothing

4. The LVA orientations should vary smoothly from one node to the next. In addition to cen-

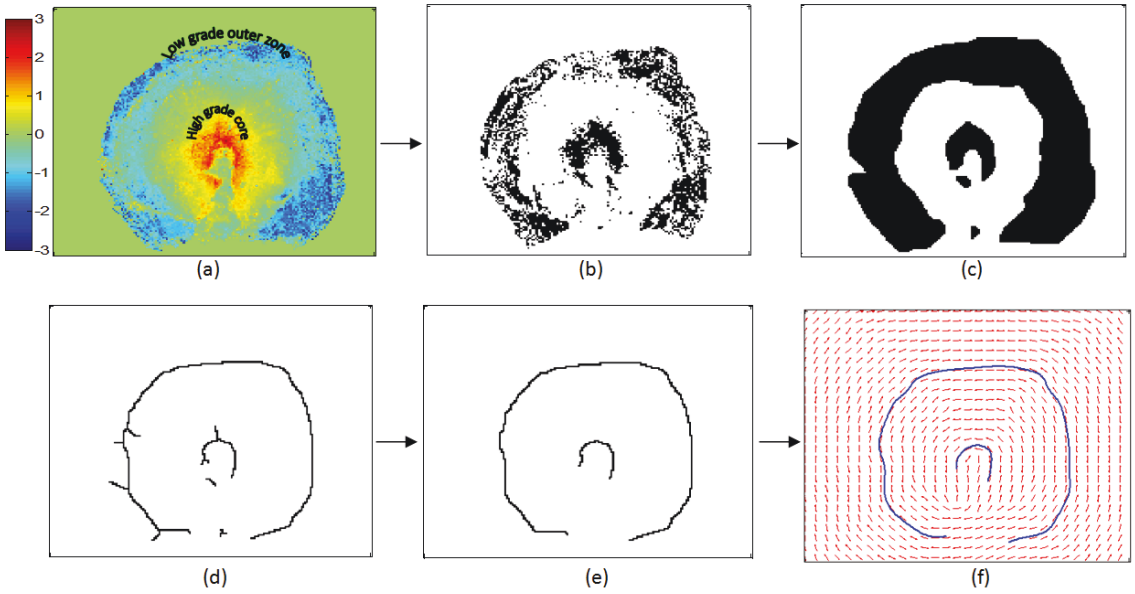

Figure 5.2: LVA field generation of a 2D layer at elevation 50 m. In the following steps first (a) examine a 2D plan section and choose cutoff values that preserve the original shape of mineralization. (b) Binary coded data is processed with image cleaning technique MAPS. (c) Smoothed image is then iteratively thinned to the centerline. (d) Irregularities such as unwarranted bifurcations in thinned centerlines are removed automatically. (e) Splines are fit to cleaned centerlines and LVA orientations are taken tangential to the splines. (f) Moving window technique is used to populate the LVA field. All plot dimensions shown are 153m$\times$180m.

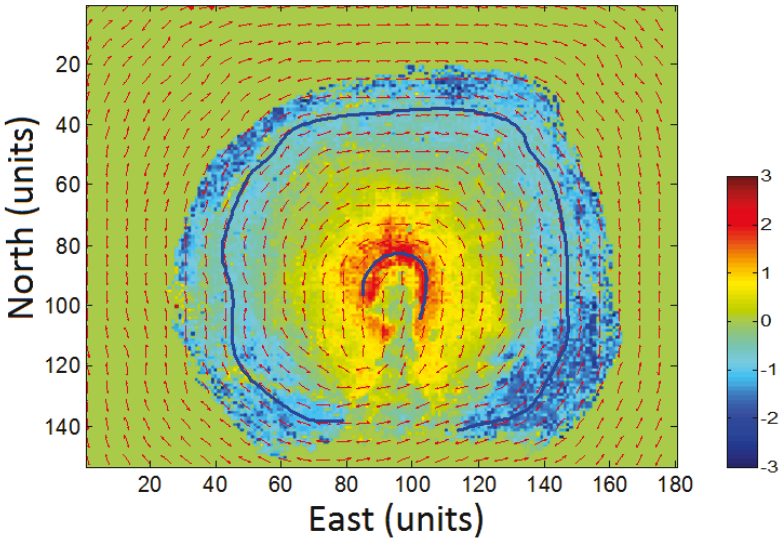

Figure 5.3: The resulting LVA field obtained at the end of thinning and centerline cleaning overlain on top of the normalized grade at elevation 50 m.

terline extraction k3m.exe fits splines and calculates the LVA orientation at each point. The direction of continuity is taken tangential to the splines.

5. The preceding steps can be performed at every bench separated by 5 or 10 m of elevation. In order to get the full 3D LVA field, the continuity of adjacent layers are interpolated by deducing local orientations around the splines and populating the LVA orientations by a moving window method

6. Incorporate the 3D LVA map into estimation with kt3d_lva.exe (Boisvert, 2010)

The smoothness of the LVA field is largely dependent on the shape representation obtained in Step 3 (Figure 5.2c). A compact object of even thickness would give well connected centerline that preserves the original topology. Trial-and-error must be used for choosing cut-off values for every 2D section examined.

It is recommended that an image smoothing filter is applied to binary coded data before centerline extraction by thinning algorithms, as the latter is very sensitive to noise especially minor distortions in the data (missing data, uneven ridges at the border pixels, etc). Gslib program MAPS (Deutsch, 1998) is applied here with a smoothing window template of 5×5. The resulting centerline is a single pixel thick and splines are fitted separately to each section. The LVA orientations

are tangential to continuity of the splines shows that both the ellipsoidal nature at the core and the radial outer region can be maintained in the LVA field (Figure 5.3). The separation of data into distinct zones is rather subjective and more areas of zonation could be considered (a zone of transition between the extremely high and low grade values). However, the idea of this study is to demonstrate a methodology for 3D analysis and provide a guide for practical issues, and so a single style of deposition is considered at low elevations and two distinct zones at higher elevations.

Several programs have been written for developing the 3D LVA field. A thinning algorithm is necessary and it is also imperative that irregularities in the thinned centerlines are identified and removed. The program k3m.exe can handle these practical considerations and outputs the parameters needed to define a 2D LVA field.

5.3 Manual Inference of the LVA Field

The important issue in the previous methodology is to arrive at skeletons or centerlines that preserve the shape of the initial structure. Alternatively polylines could be fit manually based on a practitioner's knowledge of the geology. If data clearly displays the locally varying features of interest then a polyline can easily traced along the desired structural continuity. Drill hole data may be scarce in which case a subjective model of the geology can be borrowed from an already interpreted deposition assumed to have similar heterogeneities.

Consider the 40 m elevation of the deposit (Figure 5.4). There is sufficient data to visualize the LVA features and polylines can be fitted (solid blue lines in Figure 5.4) by manually selecting points along the mineralization of interest. Splines are fit for a smoother interpolation of the LVA field.

5.4 Semi-automatic Feature Interpolation

The previous approach discussed skips the thinning altogether and manually interprets polylines where the data is densely sampled. Knowledge of the LVA that is apparent from the available data can be exploited to model the continuity in the copper porphyry.

Consider the example in Figure 5.5 of a 2D section of the porphyry data. By evaluating the plan section two distinct mineralization regions can be modeled by an inner ellipsoidal core and a surrounding radial low grade boundary. LVA orientations are the gradient of the fitted object. This way of LVA inference is effective for capturing the underlying geological feature as well as a practical means of predicting LVA at unsampled mining benches.

To generate a complete 3D LVA field these conic shapes are fit manually in 2D plan sections 10

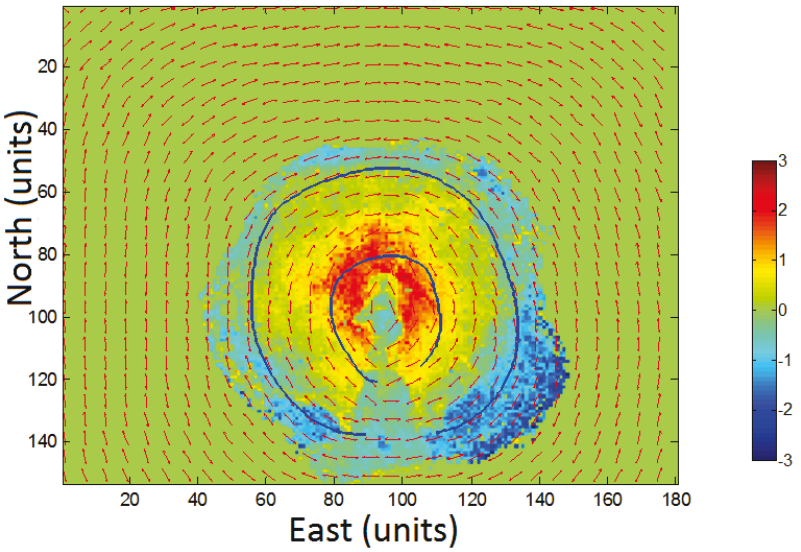

Figure 5.4: The orientation of the LVA is tangent to the manually fit line (blue) at elevation 40 m.

m apart (Figure 5.6). At these 2D sections the associated shape parameters of ellipse and circle fully define the spatial characteristics at every mining bench uniquely. Table 5.1 lists parameters of the conic objects that include the radius (R) and XY centers of coordinate (X2, Y2) of the circle at the outer low grade region, also values of semi major and semi minor axes (A,B) , and center of the longitudinal ellipsoid (X1, Y1). Linear interpolation of these shape parameters enable feature representation by LVA field for all regions between two manually interpreted plan sections and below the lowest bench.

For each 2D section the LVA field is generated using Fortran based Gslib style program sfit.exe. The program reads in the parameters of the ellipses and circles and outputs the parameters needed to define an exhaustive LVA map. The manually fit shape parameters (Table 5.1) can be easily interpolated in-between the 2D sections and also extrapolated to the bottom of the final pit. This treatment demands little professional time compared to both centerline extraction by thinning and manual polyline fitting as the shape parameters have modeling flexibility to automatically correlate the progression of the features in the vertical. Semi automatic fitting of the conic sections (Figure 5.6) allows for a less involved way to arrive at an LVA field that effectively captures the radial nature of the porphyry. Once the complete LVA field is generated for all layers estimation is done using kriging with LVA (Boisvert, 2010).

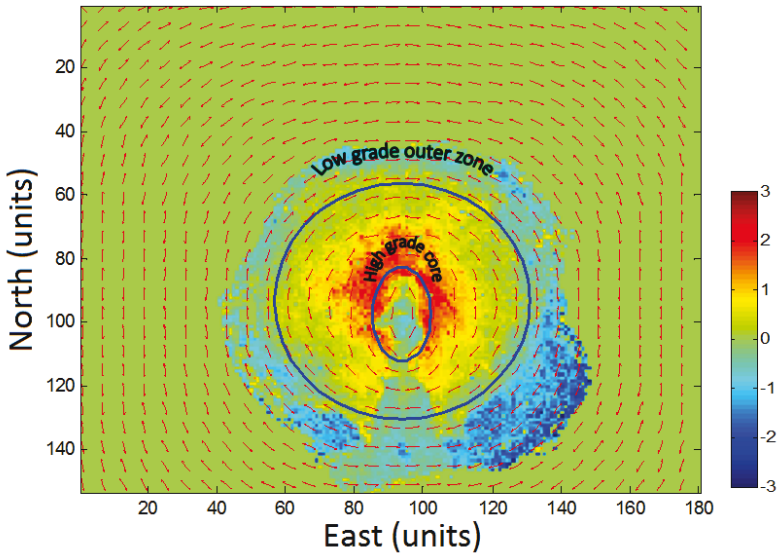

Figure 5.5: Conic shapes are fitted manually to the style of the underlying geology at elevation 40 m. Parameters to fully define the core and its circular boundary are the radii and center of coordinates of ellipses and circles, which is needed to define a 3D LVA field.

5.5 Remarks

It is important that the polylines conform to the geologic continuity of the deposit and that it is not confused with the boundary of different ore mineralization. The continuity directions of the LVA maps obtained so far emphasize the radial nature of the copper porphyry , especially the outer low grade zonation , as it gives a smooth transition from an ellipsoidal core to the change in spatial distribution at the outer boundary. Additionally, the shapes or splines fitted to the polylines have to be easy to interpolate between layers as well as extrapolate to regions where there is no data. Consider the last section where at every 10 m an ellipse and a circle was fitted, and these shape objects together have 7 parameters (centre of circle coordinates and its radius; 2 radii and center of coordinates). This method is easily to carry forward to all sections and results are given in Figure 5.6 (also see Table 5.1).

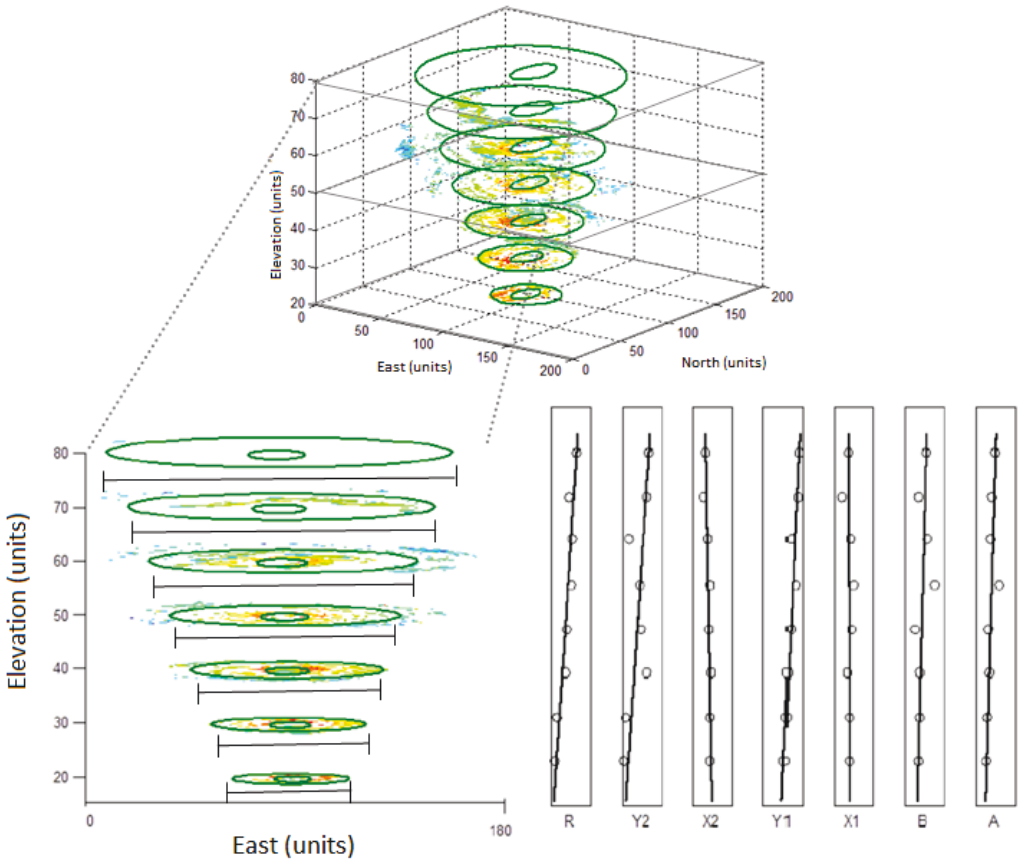

Figure 5.6: Manually evaluating underlying LVA by assigning conic shapes at selected elevations. The shape parameters need to be determined by linear interpolation for values in between the selected mining benches as well as by extrapolation to the bottom of the projected mine pit.

Table 5.1: Parameters for fitted circles and ellipses at various elevations.

Elevation (m)	R (m)	X2 (m)	Y2 (m)	X1 (m)	Y1 (m)	B (m)	A (m)
10	8.7	96.3	90.4	97.7	90.6	6.7	10.9
20	16.5	95.9	91.0	97.6	91.6	7.3	12.2
30	37.8	99.0	96.2	96.6	92.2	7.5	13.6
40	40.2	92.9	94.8	99.1	94.2	5.1	12.8
50	52.6	94.8	94.5	100.2	96.2	15.3	23.6
60	55.2	90.7	91.9	98.3	93.7	11.4	15.4
70	45.3	78.4	96.2	93.8	97.2	6.8	16.1

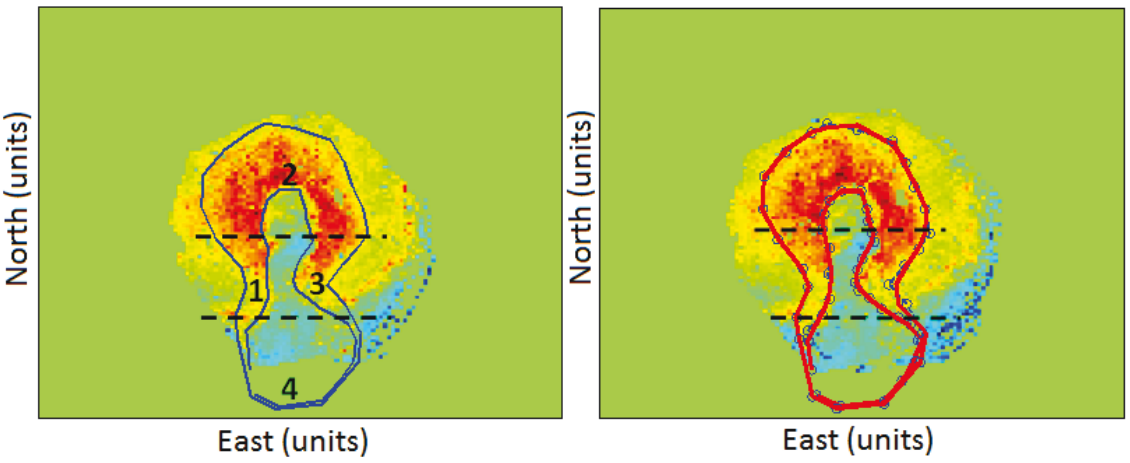

Figure 5.7: Polyline fitting from the given interpretation (solid blue line). Polynomials of sixth degree are fit to each region of the polylines shown by solid red lines (right).Plot dimensions are 153m$times$180m.

Now consider a polyline interpretation (Figure 5.7). Spline are fit at separate sections of the polylines as both the proposed inner and outer polyline cannot be modeled by a single polynomial, as the given polylines are not a one-to-one function . So starting with the section at the core, the polyline is then divided into 4 subsections and at each of these now a sixth order polynomial is fitted for a smooth interpretation. All these amount to a staggering 96 parameters that need to be interpolated. It would be very difficult to obtain a sound polyline interpolation for such an exercise.

Polylines here are utilized to outline the major directions of continuity and it is critical that they conform to the anisotropy depicted from the data. However, from the given interpretation in Figure 5.8 there are sections that suggest the anisotropy to be perpendicular to the actual feature. It is demonstrated earlier that the generation of LVA fields are critical to estimation as LVA orientations describe the way data points are correlated. So as a first step for 3D mineral characterization a continuity model has to be established that provides an adequate description of the underlying geology.

To compare how the different LVA interpretations affect the corresponding results, estimation is done using simulated drill hole data for the Cu porphyry deposit and sampling at 1226 locations. For visual inspection the estimation results are shown as 2D cross sections at several elevations (Figure 5.9 and Figure 5.10). It becomes evident that the LVA interpretation has a significant effect at lower elevations where the data density is very sparse.

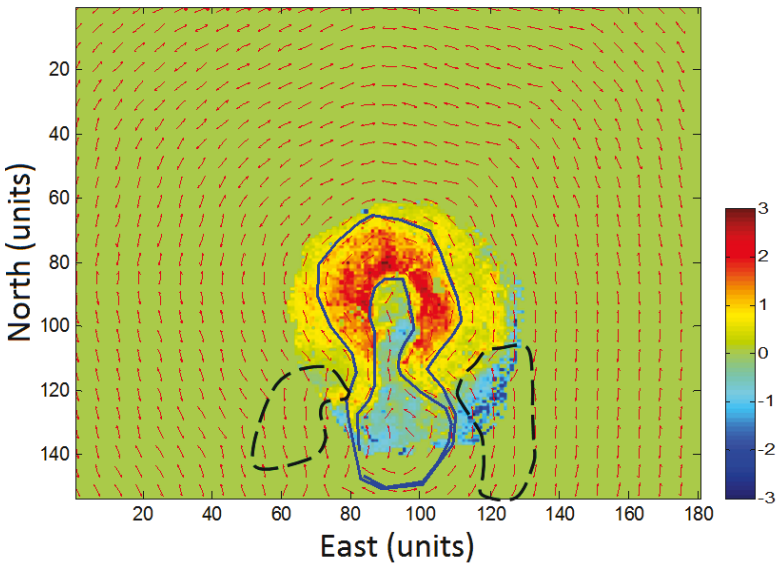

Figure 5.8: LVA field generation from the given polyline interpretation. Highlighted region in black show LVA orientations lie orthogonal to the desired continuity shown by the data.

5.6 Results and Discussion

So far the techniques for generating an LVA field is described and the several methods explored are intended to provide a guideline for evaluating similar deposit. Exhaustive 3D LVA fields are generated using the techniques discussed in this chapter and the gradient based moving window presented in Chapter 3. Results from kriging with the different LVA fields and omnidirectional kriging are compared. Cross validation of the drill hole data (Figure 5.11) suggest a 2.5% increase in correlation when kriging with LVA (manual and semi-automatic LVA field generation). Moreover compared to traditional estimation, kriging with LVA (LVA field generated with manual interpretation) has better regression fit as there is an increase of 11% in the slope of regression for estimation with LVA which is observed by the poor fit of the regression line for omnidirectional kriging. The mean square error in the case of semi-automatic LVA generation is 0.246 compared to 0.285 for omnidirectional kriging - which is significantly lower by 14.5% when examining the two techniques. Another summary statistic presented is the covariance measure between the statistics and the truth. Crossvalidation results show an improved covariance value for traditional kriging of about 5%. However, it can be argued that there are some benefits to incorporating LVA fields into modeling as the estimated map of porphyry example appear more geologically realistic.

Incorporating LVA with kriging accounts for second order non-stationarity in the domain so

there is greater accuracy in modeling conditioned to available data. Omnidirectional kriging only reproduce an indistinct shape of the desired ellipsoidal high grade core and a disjointed outer zone at lower elevation of the porphyry mine. The suit of LVA field generation methodologies discussed in this section all come with inherent subjectivity and the influence of the different LVA interpretations are apparent (Figure 5.9 and Figure 5.10). Sparsely sampled data impart limited information on LVA when incorporated into modeling, which alone however cannot honour all details of LVA in complex depositions. LVA fields are a necessary part of non-stationary estimation techniques and must be combined into geostatistical modeling.

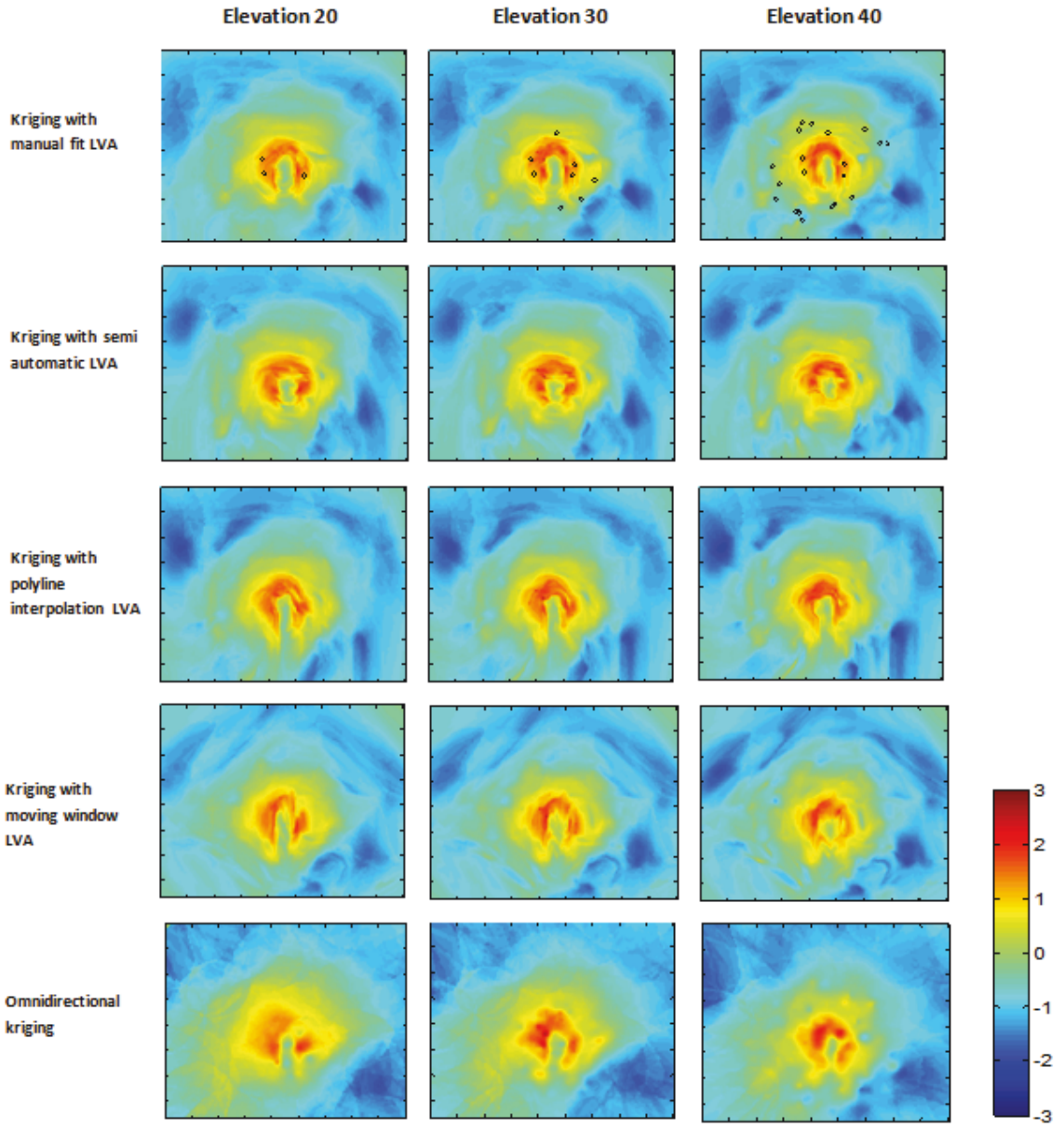

Figure 5.9: Estimation of simulated drill hole data by kriging with five different LVA field interpretations and omnidirectional kriging. Elevations near the bottom of the copper porphyry mine are shown. Plot dimensions are 153m$\times$180m.

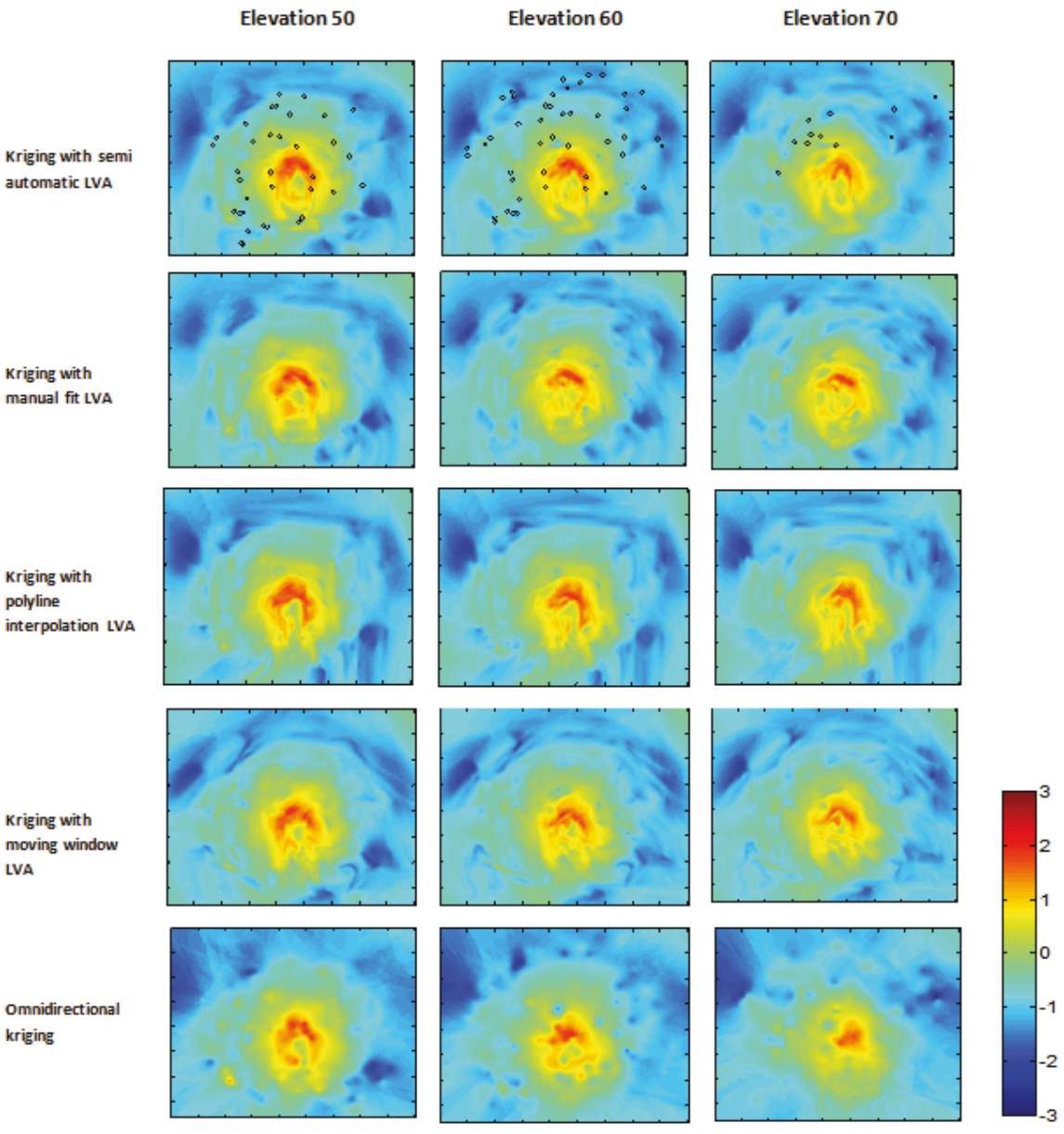

Figure 5.10: Estimation results at elevations 50m, 60 m and 70 m. All plot dimensions are 153m$\times$180m.

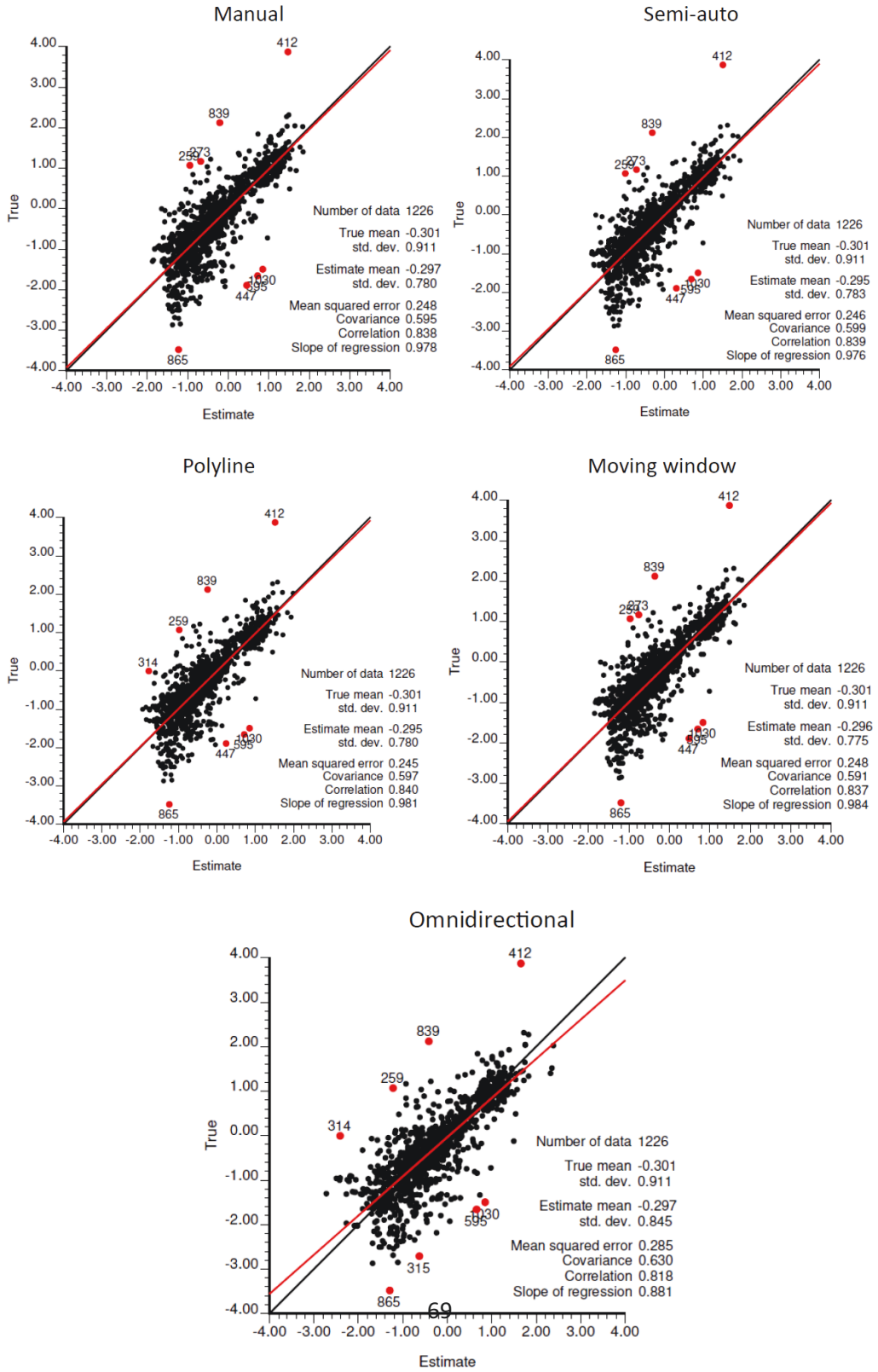

Figure 5.11: Cross validation results of estimation with simulated drill hole data.

Chapter 6

Conclusions and Future Work

An LVA field is a quantitative measure of orientation and magnitude of anisotropy. Generation of such field is dependent on available knowledge in the domain i.e. the type of data (exhaustive secondary variable, drill hole log); geological structure, scope or density of sample measurements in the domain are all contributing factors. Different data sources may need different treatments in determining a well-defined LVA field. Traditional methods such as kriging do not account for second order non-stationarity, as a result estimation of complex undulating features is often reproduced poorly. If more information on the geology is known from availability of other sources it can be used to build an exhaustive LVA field. The generation of an LVA field is a critical step for much work aimed at nonstationary geostatistics and the LVA has significant effect on end results. Kriging with LVA (Boisvert, 2010), local search reorientation (Xu, 1996; Deutsch and Lewis, 1992) are a few of the techniques that require the specifications of an LVA field for numerical modeling.

Different LVA generation techniques are presented here that evaluate various types of data. Often LVA is overlooked data available are sparse. However various sources can be used to delineate complex anisotropy including direct angle measurements at discrete points (from fullbore FMI or a practitioner's manual interpretation), geological knowledge of the deposit such as the trend of mineralization, conditioning hard and/or soft data and seismic information related to the variable of interest. Chapters 2 and 3 discussed the methodologies for the inference of LVA field from point source data, exhaustive secondary information and lastly geological bodies. The thesis contributions include programs for the generation of LVA fields from various aforementioned data types in 2D and 3D. Examples are shown alongside these different methodologies using real data when possible and synthetic data is used elsewhere.

Thesis Contributions

Information on LVA is rarely derived from limited input data. Instead LVA can be generated from additional sources that may include a practitioner's interpretation of the modeling area, geologic information from similar deposits etc and these can be imposed into modeling with nonstationary estimation techniques used alongside conditioning data. A combination of several existing and new approaches are implemented for building an LVA field from the following data sources:

1. **3D Point Data**: Direct inference of anisotropy orientation is available in some cases at discrete locations, however determining the LVA orientation exhaustively is not straightforward. In 3D often the strike and dip angles are taken which sufficiently describes most geological structures. Such data is axial and warps at 180°. Prior to estimation the data is decomposed to spherical X, Y, Z components and these are reoriented so that local orientations assume a dispersion of minimum spherical angle variance. Local estimation is done using standard kriging. In rare cases when the plunge angle is not zero a different approach is applied as the data is no longer axial. The method is to convert the conditioning data into a hypersphere entity called quaternion and to calculate an average quaternion. Transformation to quaternions is straightforward and estimation is done with inverse distance method.

2. **Exhaustive Secondary Data**: When exhaustive seismic information (i.e. geophysical surveys) of bulk properties are available that is related to the variable of interest, it can be used to generate the LVA field. This information may be exploited to determine the local orientations. Two methodologies for the LVA inference is considered that have a great deal of applications in image and texture analysis. Given an outcrop analog the first method calculates the gradient of the image and constructs a structure tensor that stores information about local orientations. In the PCA based approach the similar information is captured in an N×2 matrix. Eigenvalue and SVD decomposition gives the principal direction of continuity. Anisotropy within the geology can vary at different scales and to account for that a modified search area is implemented. A method is developed that positions ellipsoidal search neighbourhoods consistent with the scale of the feature of interest when estimating the orientation about a certain location. This facilitates the collection of gradient information about an area that best describes the style of the underlying continuity. LVA orientation can be found using both the gradient and PCA- based methods in 2D and 3D.

3. **Geological Body**: Often the geometry of a deposit aligns with the continuity of variables of interest within modeling domains. In such cases a bounded structure of the deposit can be considered to model the LVA. Existing thinning techniques are used to give the general shape representation in the form of a skeleton (medial axis) or centerline of the original structure. Splines are fit to these centerlines for a smoother approximation of the anisotropy and local orientations are taken tangential to the splines. A 2D implementation of a thinning algorithm (k3m) is implemented which takes a compact binary transformed 2D objects and outputs the coordinates of the thinned centerline. Practical considerations for identifying and removing artefacts from a thinned skeleton are met. For a complex structure the centerline extraction can give an elaborate skeleton in which case the spline fitting is done in an iterative manner.

The available geological information must be incorporated for the generation of an LVA field but in most cases there are uncertainties associated with it. For modeling any specific deposit generally there are several LVA inferences based on various data or manual inference from an expert's geologic knowledge. In this case it is necessary to combine the information on LVA into a single source which has a higher degree of confidence. A tensor based combination is presented in Chapter 4 that gathers information on local orientation from several LVA fields to give a unified orientation of anisotropy. The tensor based combination of LVA fields ensures that the change in the direction of continuity is logical and smooth, and it can handle local inconsistencies. In 2D cases spherical angle variance can be a measure to highlight inconsistent regions in an LVA field. It has been shown that the resulting combined LVA field has lower regional inconsistencies of the anisotropy vectors i.e. angle variance is lower. Chapter 6 shows that considering LVA fields can benefit the resulting estimation and lend greater geological realism into modeling by using data from copper porphyry deposit.

Future Work

The methodologies outlined above and the associated implementations provide the tools for the inference of LVA fields from separate data sources. Generation of LVA fields allows for the nonlinear complex spatial anisotropy to be quantified and it is a critical step for existing nonstationary estimation techniques. Relevant geological information must be taken into account for building an LVA field as the available sample data is scarce and rarely characterizes the underlying heterogeneities.

This work focused on building of a set of methodologies that are specific to the types of data available for generating an exhaustive LVA field. There is room for further exploration on some

details. For instance the main difficulty in dealing with point data described by three anisotropy angles was mentioned and estimation utilizes inverse distance method. It involves calculation of an averaged quaternion that represents the orientations in a transformed 4D space. It would be interesting to use kriging weights for quaternion averaging.

Another research area could look at quantifying the uncertainties associated with LVA fields. Usually with gradient and PCA based methods the associated R values give some indication of the local uncertainties. Tools and methodologies can be developed for evaluating uncertainties across any given set of LVA fields. Research can be also geared towards developing tools for easy visualization of 3D LVA fields.

References

Allmendinger, R., Cardozo, N., & Fisher, D. (2012). *Structural Geology Algorithms*. Cambridge University Press: New York.

Arpat, G., & Caers, J. (2007). Conditional simulation with patterns. *Mathematical Geology*, *39*(2), 177--203.

Boisvert, J. (2010). Geostatistics with Locally Varying Anisotropy. PhD Thesis. *University of Alberta*, 191.

Boisvert, J., & Deutsch, C. (2011). Programs for kriging and sequential Gaussian simulation with locally varying anisotropy using non-euclidean distances. *Mathematical Geology*, *37*(4), 495--510.

Caers, J., & Zhang, T. (2002). *Multiple-point geostatistics: a quantative vehicle for integrating geologic analogs into multiple reservoir models* (Tech. Rep.). Stanford University.

Cammoun, L., Castaño-Moraga, C., Muñoz-Moreno, E., Sosa-Cabrera, D., Acar, B., Rodriguez-Florido, M., … Thiran, J. (2009). *A Review of Tensors and Tensor Signal Processing*. In Tensors in Image Processing and Computer Vision, Springer: London.

Cyganek, B., & Siebert, J. (2009). *An Introduction to 3D Computer Vision Technique and Algorithms*. John Wiley & Sons Ltd: West Sussex.

De Jager, G. (2012). The influence of geological data on the reservoir modeling and history matching process. PhD Thesis. *Delft University of Technology*, 143.

Deutsch, C. (1998). Cleaning categorical variable (lithofacies) realizations with maximum a-posteriori selection. *Computers & Geosciences*, *24*(6), 551--562.

Deutsch, C., & Journel, A. (1998). *Gslib: Geostatistical Software Library and User's Guide* (2nd ed.). Oxford University Press: New York.

Deutsch, C., & Lewis, R. (1992). Advances in the practical implementation of Indicator Geostatistics. In *Proceedings of the* $23^r d$ *APCOM Symposium Tucson* (pp. 169--179).

Eriksson, M., & Siska, P. (2000). Understanding Anisotropy Computations. *Mathematical Geology*, *32*(6), 683--700.

Feng, X. (2003). Analysis and Approaches to Image Local Orientation Estimation. Master's Thesis. *University of California, Santa Cruz*, 79.

Feng, X., & Milanfar, P. (2002). Multiscale principal components analysis for image local orientation estimation. *Proceedings of the 36th Asilomar Conference on Signals, Systems and Computers : Pacific Grove*, *1*, 487--482.

Giambelluca, T., Chen, Q., Frazier, A., Price, J., Chen, Y., Chu, P., … Delparte, D. (2013). Online rainfall atlas of Hawaii. *Bulletin of the American Meteorological Society*, *94*, 313--316.

Gonzalez, R., & Woods, R. (2007). *Digital image processing* (3rd ed.). Pearson Prentice Hall: New Jersey.

Granlund, G., & Knutsson, H. (1995). *Signal Processing for Computer Vision*. Kluwer Academic Publishers: Dordrecht.

Grobekatthofer, K., & Yoon, Z. (2012). *Introduction to quaternions for spacecraft attitude representation.* (Technical Report : `http:// www.tu-berlin.de/ fileadmin/ fg169/ miscellaneous/ Quaternions.pdf`)

Hassanpour, R. (2007). Tools for multivariate modeling of permeability tensors and geometric parameters for unstructured grids. Master's Thesis. *University of Alberta*, 71.

Hassanpour, R. (2013). Grid-free Facies modeling of inclined heterolithic strata in the McMurray formation. PhD Thesis. *University of Alberta*, 181.

Haubecker, B., & Jahne, B. (1996). A tensor approach for local structure analysis in multi-dimensional images. In G. Girod, H. Niemann, & H. P. Seidel (Eds.), *3D image analysis and synthesis* (pp. 171--178).

Jahne, B. (1997). *Digital Image Processing* (4th ed.). Springer-Verlag.

Juelin, D., & Moreaud, M. (2008). Segmentation of 2D and 3D textures from estimates of the local orientation. *Image Analysis and Stereology*, *27*(3), 183--192.

Katkovnik, V., Egiazarian, K., & Astola, J. (2002). Adaptive Window size image de-noising based on Intersection of Confidence intervals (ICI) rule. *Journal of Mathematical Imaging and Vision*, *16*, 223--235.

Kopaska-Merkel, D., & Mann, S. (1992). Regional variation in microscopic and megascopic reservoir heterogeneity in the Smackover formation, Southwest Alabama. *Geological Survey of Alabama, Reprint Series 90*, *42*.

Larrondo, P., & Deutsch, C. (2004). Accounting for geological boundaries in geostatistical modeling of multiple rock types. In P. Larrondo & C. V. Deutsch (Eds.), *Geostats Banff 2004: proceedings of the* 7^{th} *international geostatistics congress* (Vol. 14, pp. 3--12).

Leuangthong, O., Khan, K., & Deutsch, C. (2008). *Solved Problems in Geostatistics*. John Wiley & Sons: New Jersey.

Lowe, D. (2001). Local feature view clustering for 3D object recognition. In *Proceedings of the IEEE computer society conference on computer vision and pattern recognition, Kauai* (pp. 682--688).

Mardia, K., & Jupp, P. (2000). *Directional Statistics* (1st ed.). John Wiley & Sons Ltd: West Sussex.

Markley, L., Cheng, Y., Crassidis, J., & Oshman, Y. (2008). Averaging Quaternions. *Journal of Guidance, Control and Dynamics*, *31*(2), 440--442.

McLennan, J. (2008). The Decision of Stationarity. PhD Thesis. *University of Alberta*, 168.

Min, P. (2011). (`http://www.cs.princeton.edu/ min/thinvox/ `)

Neufeld, C., & Deutsch, C. (2004). Angle Rotations in GSLIB. *Centre for Computational Geostatistics Annual Report 6, University of Alberta*.

Ortiz, J., & Emery, X. (2006). Geostatistical estimation of mineral resources with soft geological boundaries: A comparative study. *Journal of the South African Institute of Mining and Metallurgy*, *106*(8), 577--584.

Palagyi, K., & Kuba, A. (1999). Directional 3D Thinning using 8 subiterations. *Discrete Geometry for Computer Imagery LNCS*, *1586*, 325--336.

Saeed, K., Marek, T., Rybnik, M., & M., A. (2010). K3M: A universal algorithm for image skeletonization and a review of thinning techniques. *International Journal of Applied Mathematics & Computer Science*, *20*(3), 317--335.

Schuenemeyer, J., & Drew, L. (2011). *Statistics for Earth and Environmental Scientists*. John Wiley & Sons Ltd: New Jersey.

Shepherd, M. (2009). Predicting the geology in the gaps between the wells. *Oil Field Production Geology: AAPG Memoir*, *91*.

Strebelle, S. (2002). Conditional simulation of complex geological structures using multiple-point statistics. *Mathematical Geology*, *34*(1), 1--22.

Strebelle, S., & Zhang, T. (2005). Non-stationary multiple point geostatistical models. In O. Leuangthong & C. Deutsch (Eds.), *Geostatistics banff 2004* (pp. 235--244).

Stroet, C., & Snepvangers, J. (2005). Mapping Curvilinear structures with Local Anisotropy Kriging. *Mathematical Geology*, *37*(6), 979--988.

Sullivan, J., Satchwell, S., & Ferrax, G. (2007). Grade estimation is the presence of trends - the adaptive search approach applied to the Andina Copper Deposit, Chile. In J. Magri (Ed.),

Proceedings of the 33^{rd} International Symposium on the Application of Computers and Operations Research in the Mineral Industry, Santiago (pp. 135--143).

Tiab, D., & Donaldson, E. (2012). *Petrophysics: Theory and practice of measuring reservoir rock and fluid transport properties*. Gulf Professional Publishing: Waltham.

Wackernagel, H. (1998). *Multivariate Geostatistics* (2nd ed.). Springer Verlag: Berlin.

Wang, T., & Basu, A. (2007). A Note on a fully parallel 3D thinning algorithm and its applications. *Pattern Recognition Letters*, *28*(4), 501--506.

Wilde, B., & Deutsch, C. (2012). Kriging and simulation in presence of stationary domains: Developments in boundary modeling. In P. Abrahamsen, R. Hauge, & O. Kolbjørnsen (Eds.), *Geostatistics Oslo 2012* (Vol. 17, pp. 289--300).

Xu, W. (1996). Conditional curvilinear stochastic simulation using pixel-based algorithms. *Mathematical Geology*, *28*(7), 937--949.

Yang, Y. (2012). Spacecraft attitude determination and control: Quaternion based method. *Annual Reviews in Control*, *36*(2), 198--219.

Appendix A

Programs for LVA field generation

Fortran Program for the generation of LVA Field from Exhaustive Data

The GSLIB style program genlva.exe (Figure A.1) is developed for LVA field generation from exhaustive data. The input file contains the data which can be secondary data sourced from seismic survey, outcrop images etc. It utilizes the moving window techniques discussed earlier and calculates the structural tensor for each local neighbourhood about the node being estimated. Decomposition of local tensors provide the direction of maximum continuity and a measure of the magnitude of anisotropy termed reliability (R) can also be easily derived. It allows different options for the estimation of LVA orientation in both 2D and 3D (Lines 6-7). The moment of inertia technique (Hassanpour,2007) is included alongside gradient and PCA based implementations. However, the MOI is offered only in 2D. The number and size of the grid for the input file should be specified in Lines 9-11 which follows standard GSLIB convention.

```
1                  Parameters for GENLVA
2                   ********************
3
4  START OF PARAMETERS:
5  estusim.out                -file with data
6  1                          -option: 1=Gradient, 2=PCA, 3=MOI
7  3                          -option: 2=2D, 3=3D
8  estusim_lva.out            -file for output
9  200   1   2                -nx, xmn, xsiz
10 200   1   2                -ny, ymn, ysiz
11 10    1   1                -nz, zmn, zsiz
12 24                         -window size
13 0.1                        -ratio1(minor/major)
14 1                          -ratio2(vert/major)
15 1                          -option: use adaptive window? (0=no,1=yes)
16    30   50                   -emajor range   (2D/3D)
17    0.5  1                    -eratio1 range  (2D/3D)
18    0.5  1                    -eratio2 range  (3D)
19    0  180                    -eangle1 range  (2D/3D)
20    0  180                    -eangle2 range  (3D)
21    0  180                    -eangle3 range  (3D)
```

Figure A.1: Program for the generation of LVA field from exhaustive data

The output file contains the 5 parameters needed to define an LVA field - three angles of orientation and two ratios of the magnitude of anisotropy. Window size option (Line 12) describes the search neighbourhood and should always be an even number. This program also incorporates the adaptive window framework for analysis of features at different scales. Lines 15-21 lists the parameters needed for using the adaptive window option. In 2D a user needs to define the ranges for the semi-major, semi-minor axes and rotational band for the ellipsoidal window.

Program for the generation of LVA Field from Point Data

The standard GSLIB gridding system in used (Lines 7-9). Similar to genlva.exe, this program quat_avg.exe (Figure A.2) allows the user to define the anisotropy magnitude for the domain (Lines 11-12) which are the necessary parameters to completely describe the LVA field. Search neighbourhoods are the traditional moving window whose dimension must be specified in Line 10 and must always be an even number to maintain a square search area. Interpolation of direction angle measurements

through quaternions is implemented using inverse distance estimation. The only other input required is the power parameter for inverse distance weighting (Line 13). For this the conditioning data are given weights that are the normalized reciprocal of the distance to the unsampled location raised to a power (ω)

```
1                 Parameters for Quaternion averaging
2                 **********************************
3
4  START OF PARAMETERS:
5  3d_point_data.dat                        -file with input initial data
6  3d_point_lva.dat                      -file for output lva
7  9  1  5                               -nx, xmn, xsiz
8  15  1  5                             -ny, ymn, ysiz
9  20  1  5                             -nz, zmn, zsiz
10 20                                    -window size
11 0.1                                   -ratio1(minor/major)
12 1                                     -ratio2(vert/major)
13 2                                     -power parameter
```

Figure A.2: Program for the generation of LVA field from point data

Program for the generation of LVA Field from Geobody

GSLIB style program k3m.exe (Figure A.3) is written for the skeletonization of a 2D compact geological body. The boundaries of these structures must be well defined and the program expects that the bodies are generally well connected. Prior to thinning the geo body must be preprocessed which involves binary coding the data so that all object nodes are assigned a value of 1. If there are irregularities such as missing data, or jarring at the boundaries the object must be preprocessed with a smoothing program. Line 5 specifies the binary input file; line 6 is the output file which reports the parameters necessary to fully define a 2D LVA field. In addition to thinning k3m.exe also cleans the centerline of any artefacts and fits smooth splines for computing the LVA orientation. The grid dimensions in line 7-8 and search window size in line 10 need to be specified. An additional parameter in line 9 refers to the number of discrete nodes in the thinned skeleton that should be skipped during spline fitting and a user can select the best value by trial and error to get the desired spline fit.

```
1                  Parameters for K3M thinning
2                  ***************************
3
4  START OF PARAMETERS:
5  maps55.dat                          -file with input initial data
6  layer55.out                             -file for thinned output
7  153   1   1                             -nx, xmn, xsiz
8  180   1   1                             -ny, ymn, ysiz
9  12                                      -step
10 10                                      -window size
```

Figure A.3: Program for the generation of LVA field from Geological body

Program for the manual LVA filed interpretation

The program sfit.exe (Figure A.4) allows for the manual LVA field interpretation through fitting splines at the user defined locations. This was written specifically for generating LVA field for the porphyry example in Chapter 5. A user can include upto two separate set of points to fit splines and the desired orientations are taken tangential to the splines. A moving window technique then populates the model to give a well defined LVA field. Lines 5-7 are for the input and output files, while lines 8-9 specify the standard GSLIB grid size . The two input files correspond to the different input coordinate sets and the number of locations selected in each set should be stated in lines 10-11. The step size controls the smoothness of the spline in line 12 and local search area is in line 13.

```
1                  Parameters for Fitting Splines
2                  ******************************
3
4  START OF PARAMETERS:
5  point1.dat                          -file with input initial data1
6  point2.dat                          -file with input initial data2
7  lva_layer.dat                          -file for output
8  153  1  1                              -nx, xmn, xsiz
9  180  1  1                              -ny, ymn, ysiz
10 37                                      -number of points1
11 37                                      -number of points2
12 1                                    -step
13 4                                    -window size
```

Figure A.4: Program for the generation of LVA field from manual interpretation